

AD

RSIC-639

STUDY OF OBJECTIVES

by

J. Hartmann

Zeitschrift für Instrumentenkunde, 24, No. 1, 1-21  
and 24, No. 2, 33-47 (1904)

Translated from the German

January 1967

DISTRIBUTION LIMITED  
SEE NOTICES PAGE

# REDSTONE SCIENTIFIC INFORMATION CENTER

REDSTONE ARSENAL, ALABAMA

JOINTLY SUPPORTED BY



U.S. ARMY MISSILE COMMAND



GEORGE C. MARSHALL SPACE FLIGHT CENTER

N67-26326

FACILITY FORM 602

(ACCESSION NUMBER)	(THRU)
53	1
(PAGES)	(CODE)
<del>20-7-659</del>	23
(NAGA CR OR TMX OR AD NUMBER)	(CATEGORY)

TMX-59675

Distribution Limitation

Each transmittal of this document outside the agencies of the U. S. Government must have prior approval of this Command, ATTN: AMSMI-RBT.

Disclaimer

The findings of this report are not to be construed as an official Department of the Army position.

Disposition

Destroy this report when it is no longer needed. Do not return it to the originator.

24 January 1967

RSIC-639

STUDY OF OBJECTIVES

by

J. Hartmann

Zeitschrift für Instrumentenkunde, 24, No. 1, 1-21  
and 24, No. 2, 33-47 (1904)

DISTRIBUTION LIMITED  
SEE NOTICES PAGE

NOTE: This translation from the German language was prepared for urgent official Government use only. No verification of the copyright status was made. Distribution is limited to official recipients.

Translation Branch  
Redstone Scientific Information Center  
Research and Development Directorate  
U. S. Army Missile Command  
Redstone Arsenal, Alabama 35809

1. There is a considerable volume of literature on methods and equipment for testing of objectives; nevertheless, it appears that most of these investigations did not satisfy the strict requirements of science. One group of observers confines itself exclusively to the determination of "optical constants," namely, the focal length and the position of the principal points. They treat the lens system entirely as a mathematical form, without taking into consideration at all the aberrations connected with any lens, or else they consider these errors only an unwelcome disturbance in the accuracy of their measurements. I do not wish to go into these methods in detail here, but merely to bring to attention two errors which are frequently repeated in these measurements. The first is the locating of the image site by the setting of some mark or other on the "sharp" image of an object and the second is the use of short collimators as a substitute for an infinitely distant object. The danger of measuring a distance by sharp imaging has been repeatedly shown in other quarters, such as in the pertinent discussions which Mr. Czapski has published in *Zeitschrift für Instrumentenkunde*. The errors which can occur through improper setting of collimators have not been adequately taken into account, it would appear. Various observers note expressly that a "small collimator" is a part of their optical equipment. If it is assumed that this collimator is set in error by only 1 mm for a 25-cm length, then an error of 4 mm would be caused in focus setting of a lens of 50-cm focal length.

2. A second group of objective studies directly tests the performance of the system involved in the application for which it is intended. Thus, photographic objectives are tested by sample photographs, microscope systems by suitable test specimens, and astronomic telescope objectives by observations of double stars. Of course, this final test of the overall performance capability of the system can never be dispensed with. Since it primarily involves the judgment and not least of all the skill of the observer, it is desirable to use, in addition to these subjective evaluations, an objective type of study the result of which is given in a series of numbers or curves which make possible a safe comparison with other systems of the same type. It may be mentioned, for example, that there is great uncertainty over the performance of the large refracting telescopes of various observatories; this could be immediately eliminated by a numerical evaluation of the properties of the objectives involved.

It is not necessary to go further into the benefits that optical technology would draw from the use of exact measurements for measurement of residual aberration of objectives, because Dr. Lehmann has already described this in several publications in *Zeitschrift für Instrumentenkunde*. In a purely commercial sense, the numerical

evaluation of the properties of an objective is very desirable, because hitherto it has not been possible in the procurement of large objectives to come to agreement with the manufacturers on simple and clear conditions on whose fulfillment the contract could be made dependent. Thus, for example, the pertinent section in the contract concluded with Alven Clark for supply of the 36-inch objective for the Lick Observatory read as follows:

"The definition of the glass should in every respect be not less than that of the 26-inch aperture objective which was supplied by Clark for the Naval Observatory in Washington, and the luminance in respect to absorption in the glass should be greater in relation to the greater aperture."

Thus, only a lower, and obviously too low, limit could be established for the performance of the objective furnished, and delivery had to be made dependent upon the judgment of some observers. It is clearly seen how deficient such a process had to be for both parties, and yet up to now it has been the only one possible. If exact methods are available for measurement of residual aberration, then a limiting value for the permissible error can be agreed upon with the supplier of the objective; and after the objective is finished it can be determined with absolute certainty whether or not the requirements set up have been met. In addition, this measurement of the error can be made directly in the shop; Clark had to set up a costly mount to test the 36-inch lens in the sky.

3. The first step in establishing precise methods of this type for the measurement of objective errors was done by H. C. Vogel<sup>1</sup> in 1880, with the publication of his method for determination of chromatic aberration with the aid of the eyepiece spectroscope. Since the Vogel method has generally established itself, it has no longer been possible to be in doubt over the position of the color curve of an objective. However, the amount of the second error coming into consideration in telescope objectives (namely, that of spherical aberration or zonal aberration) is still completely uncertain. The only data on the amount of spherical aberration are based on the theoretical calculation of objectives, and it had to be assumed for this that it is extremely small in comparison with chromatic aberration. Thus, Bessel, for example, calculated the following differences in intersection distances for the Königsberger heliometer objective<sup>2</sup>:

<u>Height of Incidence</u>	<u>Spherical Aberration (mm)</u>
0.00	0.000
0.25	-0.013
0.50	-0.039
0.75	-0.064
1.00	-0.100

Because of the small amount of this error theoretically found, probably no effort has ever been made to measure it accurately. Of course, in the Foucault method<sup>3</sup> the opticians had a method of perceiving small differences in intersection distances, although this was never used for actual measurement of the error, any more than the method given by Schroeder<sup>4</sup>.

The Abbe focometer<sup>5</sup>, which permits direct measurement of focal length for various zones, is the only one of the older instruments which appears suitable for determination of the zonal aberration of objectives. However, as can be seen from Mr. Czapski's paper, this instrument, too, has been used only for determining the "fundamental value" of the focal length (namely, that for the center of the objective) and not for the determination of zonal aberration. The latter application will be mentioned again further on.

In the following, a complete study of a telescope objective with the aid of the method developed by the author in 1899, using extrafocal measurement, will be made for the various types of application. An initial brief description of this method was given in *Zeitschrift für Instrumentenkunde* (Vol. 20, 1900, p. 51), and large-scale investigations were made, using this, by Wilsing<sup>6</sup>, Eberhard<sup>7</sup>, and Lehmann<sup>8</sup>.

## I. TEST OF A TELESCOPE OBJECTIVE

4. The author understands the test of a telescope objective to be the determination of its focal length, chromatic and spherical aberration, or zonal aberration and astigmatism on the axis. To this might be added testing for extra-axial images, transmittance of the glass, and measurement of the free aperture, as well as possible notes on the position of reflex images, on centering and purity of the lenses, and similar matters. For the time being, nothing will be said about these additional properties.

The test of a small objective of 80-mm aperture and 1-m focal length with the aid of terrestrial light sources will first be described,

and the small modifications of the method which are necessary in the testing of astronomical objectives with the aid of stars will be given. The test is performed in the actual mounting of the objective, which in the case at hand is a brass tube. To the eyepiece of this tube can be connected, by means of a bayonet joint, a filar micrometer, a photographic camera, or a small slit spectrograph. The setting can be read to 0.1 mm with a vernier.

The study of the objective can be broken down into two parts:

- 1) Determination of the position of the focal points of all rays in terms of the graduation of the adjustment. This is called focusing.
- 2) Measurement of the distance of this graduation, either from a fixed point of the objective mount—which gives the combining distances—or from the second principal point of the objective, in which case the focal lengths are obtained.

#### A. FOCUSING BY EXTRAFOCAL MEASUREMENTS

5. The totality of all rays which enter the objective parallel to the axis is infinite in three ways. If the height of incidence of a ray (and thus its distance from the axis) is called  $r$ , the angle between the radius  $r$  and an arbitrarily chosen zero direction is called  $\phi$ , and the wavelength is designated as  $\lambda$ , then any axially parallel ray is completely defined by the three quantities  $r$ ,  $\phi$ , and  $\lambda$ . The task of objective testing now in short consists of complete determination of the ray path as a function of the three arguments  $r$ ,  $\phi$ , and  $\lambda$ . For this purpose it is first necessary to isolate such an individual ray,  $r$ ,  $\phi$ , and  $\lambda$ , from a ray bundle incident on the objective and then to determine its position in the image space. The ray is isolated by setting before the objective an aperture with a small opening at the point  $r$ ,  $\phi$  and permitting monochromatic light of wavelength  $\lambda$  and parallel to the axis to enter through this opening. To determine the position of the refracted ray in the image space, its intersection points with two arbitrary planes perpendicular to the axis are determined; this is the basis of the method of extrafocal measurements. As is seen, this method is not confined to objectives but can also be used with any desired optical equipment. However, the form of the aperture and the nature of the measurements in the two intersection planes will be different, depending upon circumstances. In general, the central ray  $r = 0$  is allowed to enter the system along with ray  $r$ ,  $\phi$ , and then the coordinates of the point  $r$ ,  $\phi$  are measured at the two planes with respect to the axial point, either in rectangular or in polar coordinates. The orientation of the system must be determined in a suitable manner each time. In a spectrograph,

rectangular coordinates are measured parallel to the principal section (direction of the spectrum) and perpendicular thereto (direction of the spectral lines), and in the study of the extra-axial images of an objective, rectangular coordinates in the meridional and sagittal direction are used.

6. In the testing of the axial image of a centered system, polar coordinates simplify the measurements. In such a system it may be assumed that two rays,  $r, \varphi$  and  $r, \varphi + 180^\circ$ , symmetrical to the axis, intersect on the axis as long as they remain in the meridian plane defined by the direction  $\varphi$ . Therefore, in this case it is no longer necessary to measure the positional angle in the two intersection planes, and instead of measuring the distance of each individual ray from the center ray, the distance of the two rays  $r, \varphi$  and  $r, \varphi + 180^\circ$  from one another can be determined. In this simplest case, the extrafocal measurement takes the following form. An aperture which has two openings on a diameter symmetrical to the center of the objective is placed before the objective. Then the measuring plane (and thus either the cross-hair plane of the micrometer or the photographic plate) is brought successively to the two positions  $E_1$  and  $E_2$  (Figure 1) near the intersection point  $O$  of the two rays, and the two distances  $e_1$  and  $e_2$  of the unfocused images appearing in the planes  $E_1$  and  $E_2$  are measured. If  $A_1$  and  $A_2$  are the readings corresponding to positions  $E_1$  and  $E_2$ , made at the millimeter graduation of the eyepiece adjustment, then the reading  $A$  corresponding to the focus  $O$  of the rays in question is found from

$$A = A_1 + \frac{e_1}{e_1 + e_2} (A_2 - A_1) . \quad (1)$$

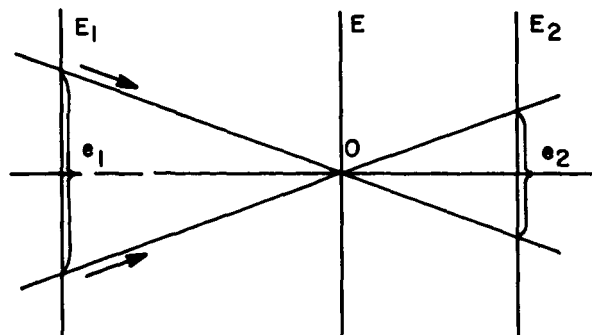


Figure 1



The values of A thus found are called  $\varphi A_{\lambda}^r$  to indicate their dependence on the three arguments r,  $\varphi$ , and  $\lambda$ .

7. It is now important to bring the apparently very extensive effort of determination of all  $\varphi A_{\lambda}^r$  values into as simple a form as possible. If the quantity A is a function of  $\varphi$  at constant r and  $\lambda$ , the system has astigmatism on the axis. As is well known, this causes the combining distance to be a minimum at a definite meridian intersection  $\varphi = \varphi_0$ , and a maximum at the perpendicular  $\varphi = \varphi_0 + 90^\circ$ . Accordingly, A can be represented in the form:

$$\varphi A = \varphi_0 A + a \sin^2 (\varphi - \varphi_0) \quad (2)$$

in which a is the amount of astigmatism, the difference between the maximum and minimum value of A. It follows from Equation (2) that

$$\varphi + 90 A = \varphi_0 A + a \cos^2 (\varphi - \varphi_0)$$

so that

$$\frac{1}{2} (\varphi A + \varphi + 90 A) = \varphi_0 A + \frac{a}{2} \quad (3)$$

This equation shows that the mean value free of the influences of astigmatism is always obtained between the minimum and maximum A, if the mean is taken from two values whose position angle  $\varphi$  differs by 90 degrees. Therefore, to find the mean value of A valid for each zone of the objective, it is not only necessary to place the holes in the aperture on one diameter but also on two mutually perpendicular diameters and at distance r from the center. It can be easily shown that not only the mean of two but also of three or any number of equidistant meridian intersections always gives the same mean value free of astigmatism, and it is useful for an understanding of the pattern of astigmatism to use more than four openings for at least one zone of the objective in this manner.

8. If the investigation is conducted photographically, then to eliminate the need for two new pictures for each zone, an attempt is made to combine in a single aperture the openings necessary for all zones of the objective. This is always possible with better objectives. Only in systems with very great zonal aberrations do the rays of the different zones pass each other near the focal point in a way requiring the use of two separate apertures. Distances e are measured directly with a filar micrometer, so it is not advantageous to combine too many holes in one aperture. For adequate separation of the images for zones

of small  $r$ , the distance of the planes E from the focal points must be fairly large. If the holes for the outermost zones have been made in the same aperture, then fairly long distances must be measured with the micrometer; this can be avoided if a special aperture is used for the outermost zones.

The diameter of the openings should be chosen between  $1/200$  and  $1/400$  of the focal length of the objective to be studied. The smaller the openings, the larger and more indistinct are the image disks to be measured, making sharp focusing more difficult. If the openings are very large, then the objective can be divided into only a few different zones; and thus the curve of zonal aberration cannot be determined exactly.

The aperture, shown half scale in Figure 2, which the author used in the photographic investigation of the objective in question, can be immediately understood from what has been said above. It was made of heavy writing paper and contained the following openings:

On the diameter $\varphi = 0^\circ$ and $90^\circ$	$r = 10, 18, 26, 38$ mm
22.5 and 112.5	$r = 30$
45 and 135	$r = 6, 14, 22, 34$
67.5 and 157.5	$r = 30$

The center points of the openings are first plotted with compass and ruler and then a 3-mm radius circle is drawn about each of these points with a small compass. This serves as center in the mounting of a punch with which the 4-mm diameter holes are punched out. The four innermost holes, which can be put in afterwards, are of 3-mm diameter. It may further be observed that it is not important for the holes to be located with mathematical exactitude, because the dimensions of the aperture do not enter the calculation. It is more important that the openings be round and smooth-edged, because otherwise the images would be irregular and difficult to measure.

9. If two extrafocal photographs are taken in monochromatic light of wavelength  $\lambda$ , with the aperture described, their measurement gives the values of  $A_\lambda$  free of astigmatism for nine zones of the objective and thus the curve of zonal aberration. In addition, the zone  $r = 30$  mm, measured on four diameters, gives an exact determination of astigmatism, the amount and location of which can be checked with the other values. This completely determines setting A as a function of the argument  $r$  and  $\varphi$  for the wavelength  $\lambda$ . To determine it as a function of  $\lambda$ , meaning the color curve, this investigation can be made

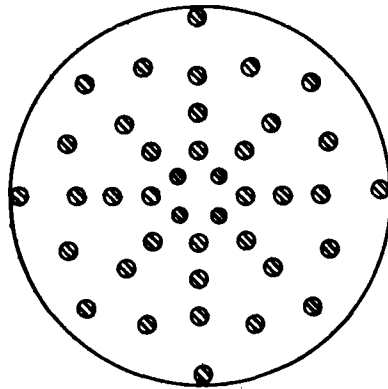


Figure 2

for a large number of different wavelengths, giving curves or tables from which the amount of A for any values of  $r$ ,  $\phi$ , and  $\lambda$  can be found. To determine the color curve in this manner, a series of monochromatic light sources is necessary. This was furnished through interposition of suitable filters before a mercury arc lamp. The filters<sup>9</sup> used were of the following type:

For $\lambda = 365 \mu\mu$	methyl violet + nitrosodimethyl aniline
405	methyl violet + quinine sulfate
436	cobalt glass + askulin solution
492	guinea green + quinine sulfate
546	true green + chrysoidine
579	eosine + chrysoidine

Some of these filters are used as solutions in cells and some were made with bath plates two by two with the films, joined by adhesion along the edge. The principle in the grouping of these filters is simply that a number of colors with absorption bands as steeply descending and as strong as possible are chosen and then so combined that only the desired narrow region of the spectrum is allowed to pass. The filters are not used for greater wavelengths than given above, because for this part of the spectrum the color curve is more conveniently determined by optical methods, making the filters unnecessary.

The described method of deriving the color curve by a series of individual photographs in monochromatic light is somewhat laborious, however, and it is more convenient to arrange the observation method for this purpose in the manner described further below.

10. If white light instead of monochromatic light passes through the two aperture openings  $r, \varphi$  and  $r, \varphi + 180^\circ$ , then at the two planes  $E_1$  and  $E_2$  short spectra occur, as a result of chromatic aberration of the objective, instead of round image points. As a simple reflection shows, that color which has the shortest combining distance occurs at plane  $E_1$  and thus inside the focus (in terms of the optical axis). This color is on the outside in plane  $E_2$ . Since in the hitherto common achromatization of two-lens objectives, that color for which a good ray combination is sought always has the shortest combining length, the short spectra in plane  $E_1$  will always be strong in light on the inner side and sharply delimited, while toward the outside it gradually decreases, so that a pear-shaped figure with a point directed outward results. In plane  $E_2$  the peak points inward. The photograph reproduced in Figure 3 shows this pear shape (inside the focus) very clearly; the well-rounded figures of the photograph of Figure 4 made in monochromatic light should be compared with this.

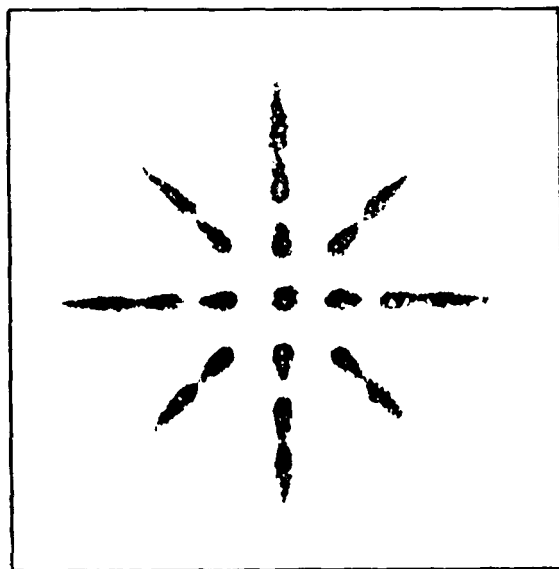


Figure 3

If a star is used as the light source in the testing of an astronomic objective, then white light must always be used. However, in this case several expedients allow the pear shape of the images to be suppressed somewhat, so that the photographs can be readily measured. To do this, the photographic plate and the star are so chosen that the maximum of the light effect falls nearly on the point of inflection of the color curve of the objective studied. If the objective is achromatized for

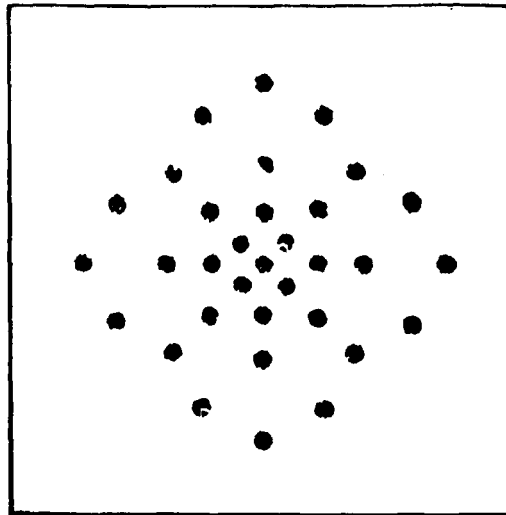


Figure 4

photographic purposes in the blue part of the spectrum, then an ordinary silver bromide plate and a star with intensive blue light (I type) is used (for example, Alpha Lyrae). If, on the other hand, an optical objective is involved, then a star which contains very little blue light (for example, Alpha Orionis) is chosen and the photographs are made on a plate type which is principally sensitive to the yellow (for example, the Peranto plate of Perutz). In this way, the zonal aberrations are obtained not for a given wavelength but only as a mean value for the colors best combined by the objective.

11. The uncertainty arising in the measurement of the pear-shaped images is completely avoided if the white light is split by a prism, either before the objective or behind the measuring plane. An exact determination of the color curve is obtained in this manner. Splitting before the objective, in which case the prism is used in the manner of the objective prism, can generally be used only for smaller objectives, because for a large objective a suitable objective prism is generally not available. This method will again be described in the study of a small objective. Splitting behind the measuring plane can be done in two ways: by photographic measurement through a slit spectrograph and by optical observation through an eyepiece prism. Both methods have proven effective and have been used widely.

The spectrograph\* is so fastened to the eyepiece mount that its collimator axis coincides with the principal axis of the objective to be tested and its slit is directed parallel to the line joining two holes in the aperture. It then lies on the long axis of the pear-shaped images (cf. the discussion in Dr. Lehmann's work<sup>10</sup>). Each of these images is then drawn out into a curved spectrum; then the intervals  $e$  of the individual spectral colors can be measured exactly. Care must be taken that the spectrograph is sufficiently free of astigmatism and thus sharply images edges lying perpendicular to the slit (for example, the dust particles in the slit). In addition, its aperture must be large enough to be able to accept completely the two bundles coming from the aperture opening. It is not necessary here that it be free of distortion and thus image a given length of the slit in all colors in the same size.

This method is the most reliable in the testing of astronomic objectives with the aid of stars. To eliminate the necessity for preparing special photographs for each zone of the objective, the openings for two zones can be combined on each aperture. Then when a star of the first spectral type is used, photographs of the type shown in Figures 5 and 6 are obtained. As is seen, these photographs show the lines of the spectrum in full sharpness, and it is merely necessary to measure the distance of two corresponding spectra for each of these lines to obtain an exact determination of the color curve. Each of these curved spectra is directly identical with the color curve shown to suitable scale.

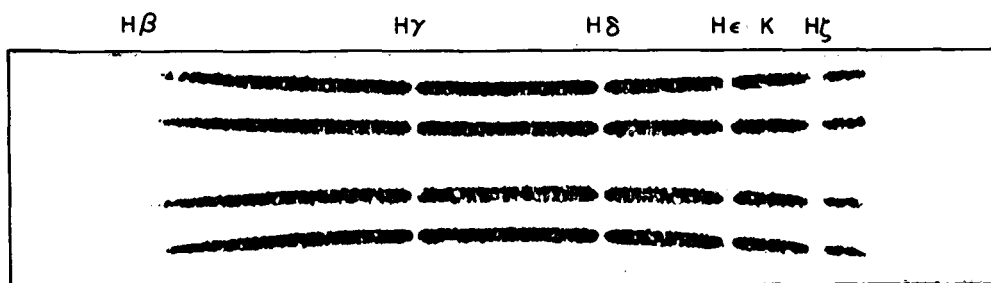


Figure 5

\*A small and very light spectrograph for this purpose is made by L. Toepfer and Sohn in Potsdam.

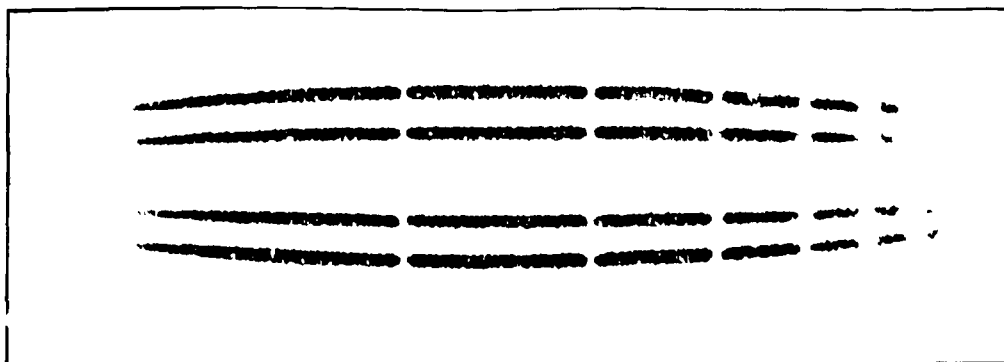


Figure 6

Since it is occasionally difficult to bring the slit exactly into the axis of the pear-shaped images, it is advantageous here to use another form of aperture opening. The aperture can be so constructed as to leave open the entire zone between radii  $r$  and  $r + \varrho$ , where  $\varrho$  is again about  $1/300$  of the focal length. Then the slit has to be arranged so that it passes exactly through the center point of the annular extrafocal image. This can be easily done if the slit plane is focused beforehand and the punctiform images formed there are brought into the slit. By turning the spectrograph about the optical axis, the aberration in the various position angles  $\varphi$ , and thus the astigmatism, can be studied.

If the slit does not exactly form a diameter of the rings in this aperture form but only a chord in them, the results will be erroneous. To avoid this danger it is better to use aperture openings shaped as two parallel slits. Figure 7 shows in full scale an aperture of this type, used for an objective of 40-mm aperture for simultaneous determination of the color curve for the two zones  $r = 8.5$  mm and  $r = 17.5$  mm. The slit here is set on direction AB.

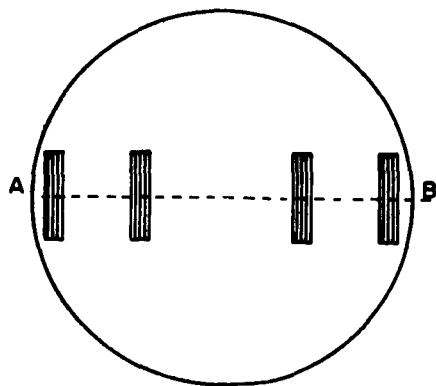


Figure 7

12. Direct optical measurement of the color curve is done in a very similar manner. For this, apertures with small round openings (as in Figure 2) are used, but in each aperture only the two corresponding openings are placed in one diameter. For simultaneous determination of the color curve of two zones, four openings can be used. A larger number of openings would confuse the eye in the spectral resolution of the light. Before the eyepiece of the micrometer is fastened a small straight prism piece. It is turned so that its principal section is parallel to the measuring hair of the micrometer, which when seen through this prism appears to be completely sharp. The aperture is so placed before the objective that the diameter containing the openings is parallel to the refracting edge of the eyepiece prism. The extrafocal images of a remote punctiform light source then appear in the field of view again as arcuate spectra of which the intervals at points of individual spectral lines are measured with a micrometer.

13. To determine zonal aberration and astigmatism by the above-mentioned measurements, leading directly to a knowledge of the color curve, it would be necessary to make the measurements for all zones of the objectives and in at least two position angles, which again would appear to be fairly laborious. Therefore, it is better to combine measurements of the latter type with the determination of zonal aberration described in Section 8, in the following manner.

If it can be assumed that the color curve has the same form for all zones of the objective, that is, that the spherical difference of chromatic aberration is zero, it is sufficient to determine the color curve for only one zone and zonal aberration and astigmatism for only one wavelength. Since the extrafocal measurements permit the difference mentioned to be measured accurately, however, it would be more correct where greater accuracy is demanded to make this also a subject of the investigation.

The next approximation results from the assumption, which is probably permissible in all cases, that the chromatic difference between two given zones is proportional to the amount of chromatic deviation for all colors. If two wavelengths for which the zonal aberration is determined directly in monochromatic light in accordance with Section 8 are designated as  $\lambda_1$  and  $\lambda_2$ , and a zone for which the color curve has been established by  $r_1$ , according to Sections 11 or 12, then with the last assumption, in general:

$$A_{\lambda}^r = A_{\lambda_1}^r + \frac{A_{\lambda_2}^r - A_{\lambda_1}^r}{A_{\lambda_2}^{r_1} - A_{\lambda_1}^{r_1}} \left( A_{\lambda}^{r_1} - A_{\lambda_1}^{r_1} \right) . \quad (4)$$



In this, all  $A_{\lambda_1}^r$  and  $A_{\lambda_2}^r$  values can be taken directly from the two zonal aberration curves and all  $A_{\lambda}^{r_1}$  values directly from the color curve.

If, on the other hand, as is the case generally in astronomic objectives, the zonal aberration has been determined for only one color  $\lambda_1$  (perhaps also for white light, cf. Section 10) and the color curve for two zones  $r_1$  and  $r_2$ , then the assumption can be made that the form of the color curve changes uniformly as  $r$  increases. This leads to the equation:

$$A_{\lambda}^r = A_{\lambda}^{r_1} + \left( A_{\lambda_1}^r - A_{\lambda_1}^{r_1} \right) + \left\{ \left( A_{\lambda}^{r_2} - A_{\lambda}^{r_1} \right) - \left( A_{\lambda_1}^{r_2} - A_{\lambda_1}^{r_1} \right) \right\} \frac{r - r_1}{r_2 - r_1}, \quad (5)$$

in which all  $A_{\lambda}^{r_1}$  and  $A_{\lambda}^{r_2}$  values are taken from the two color curves and the  $A_{\lambda_1}^r$  values from the curve of zonal aberration.

The effort expended is exactly the same whether calculation is done according to Equation (4) or Equation (5). Three series of extrafocal measurements must be made in each case to obtain the knowledge, given through the above equations, of  $A$  for arbitrary values of  $r$  and  $\lambda$ ; and this completely solves the purpose of the focusing.

For the time being, no notice can be taken of astigmatism and, therefore, of the dependence on  $\phi$ . This has no influence on the differences of two similarly determined  $A$  values appearing on the right in Equations (4) and (5). This is confined to the first principal terms  $A_{\lambda}^r$  and  $A_{\lambda_1}^{r_1}$  of the right sides. From what was said in Section 7, all the  $A$  values obtained in determination of zonal error, and thus also  $A_{\lambda_1}^r$  in Equation (4), are completely free of astigmatism; this equation thus gives an  $A_{\lambda}^r$  value free of astigmatism. On the other hand, the  $A$  values found in the measurement of the color curve, if the measurement was not made in two position angles differing by 90 degrees, are still affected with astigmatism. Therefore, the  $A_{\lambda}^r$  value found from Equation (5) is directly valid for the same position angle in which  $A_{\lambda_1}^{r_1}$  was measured. Since the astigmatism is known,  $A_{\lambda}^r$  can be easily freed from its influence.

If the above-mentioned neglect of spherical difference of chromatic aberration is permitted, the process is simplified considerably, because then a single measurement of zonal aberration suffices for each color  $\lambda_1$ , and one color curve suffices for a zone  $r_1$ . Thus in Equation (4):

$$A_{\lambda_2}^r - A_{\lambda_1}^r = A_{\lambda_2}^{r_1} - A_{\lambda_1}^{r_1},$$

and this transforms into:

$$A_{\lambda}^r = A_{\lambda_1}^r + \left( A_{\lambda}^{r_1} - A_{\lambda_1}^{r_1} \right) . \quad (6)$$

In Equation (5),

$$A_{\lambda}^{r_2} - A_{\lambda}^{r_1} = A_{\lambda_1}^{r_2} - A_{\lambda_1}^{r_1} ,$$

exactly coinciding with Equation (6), and again:

$$A_{\lambda}^r = A_{\lambda}^{r_1} + \left( A_{\lambda_1}^r - A_{\lambda_1}^{r_1} \right) .$$

14. The exactness of extrafocal focal point determination results from the following considerations. It will be assumed that  $\alpha$  is the mean error of a reading on the eyepiece draw,  $\epsilon$  the mean error of a measurement of the distances  $e$ , and  $\Delta$  the mean error of the resultant value of  $A$ . In addition, the abbreviations

$$w_1 = \frac{e_1}{e_1 + e_2} \quad \text{and} \quad w_2 = \frac{e_2}{e_1 + e_2}$$

are assumed.

From the basic equation, (1) with

$$\frac{A_2 - A_1}{e_1 + e_2} = \frac{F}{2r} ,$$

in which  $F$  is the focal length and  $r$  is again the radius of the zone,

$$\begin{aligned} \frac{\partial A}{\partial A_1} &= w_2 & \frac{\partial A}{\partial A_2} &= w_1 \\ \frac{\partial A}{\partial e_1} &= \frac{F}{2r} w_2 & \frac{\partial A}{\partial e_2} &= -\frac{F}{2r} w_1 . \end{aligned}$$

There is accordingly obtained:

$$\Delta = \sqrt{w_1^2 + w_2^2} \sqrt{\alpha^2 + \frac{F^2}{4r^2} \epsilon^2} . \quad (7)$$

If the two test planes are chosen almost symmetrically about the focus, then

$$w_1^2 + w_2^2 = 1 - 2w_1w_2$$

is always very nearly 1/2. There is obtained, for example:

$w_1$	$w_2$	$1 - 2w_1w_2$	$\sqrt{w_1^2 + w_2^2}$
0.5	0.5	0.50	0.707
0.4	0.6	0.52	0.721
0.3	0.7	0.58	0.761

It is thus possible to assume with sufficient accuracy:

$$\sqrt{w_1^2 + w_2^2} = 0.75 \quad .$$

Because for  $A_1$  and  $A_2$  the setting can be made on full graduations of the scale, there can be assumed approximately:

$$\alpha = 0.02 \text{ mm.}$$

For moderately good images,  $\epsilon$  is about 0.008 mm and with very good images it is about 0.003 mm, while  $F/2r$  is between 10 and 100. Because of this large factor,  $\alpha^2$  can almost always be neglected in comparison with the term  $(F^2/4r^2)\epsilon^2$ . There is then obtained instead of the strict error equation, Equation (7), the simpler expression:

$$\Delta = 0.37 \frac{F}{r} \epsilon \quad * \quad (8)$$

If  $\epsilon$  is assumed to be 0.008 mm, then the following values of  $\Delta$  result. In comparison with these are listed (Table I) the figures derived by Dr. Lehmann<sup>11</sup> from his measurements.

---

\* Professor Wilsing reports that on page 14 of his work<sup>6</sup> in the equation given by him,

$$r_x = r_m \frac{x}{m} \sqrt{\frac{3}{2}} \quad ,$$

$\sqrt{1/2}$  should be used instead of  $\sqrt{3/2}$ ; this is then identical with Equation (8) above.

Table I

$\frac{F}{r}$	$\Delta$ (mm)	Lehmann (mm)
23	0.069	0.079
26	0.078	0.074
38	0.114	0.154
56	0.168	0.171
116	0.348	0.376

As is seen, the course of Dr. Lehmann's figures agrees well with the calculation. Further data on the accuracy of the method are given below with the author's measurements.

It is seen from Equation (8) that the accuracy of focus determination through extrafocal measurement depends not upon the focal length of the objective but only upon the aperture angle of the zone involved. Thus, other circumstances being equal, the focus is found with the same linear accuracy for large as well as for small focal length; thus, this method gives results of the highest accuracy, especially for large objectives in which the linear value of aberrations is large. When stars are used in the study of astronomic objectives, there is a small loss of accuracy because of the flicker of the star images, something which should not be left unmentioned.

15. It is understandable, of course, that the small aperture openings, especially when many of them are combined on one aperture, produce a complicated refraction image near the focus. This would be very difficult to study mathematically. However, if the measuring plane is removed gradually from the focal point, then this total image degenerates, as experience shows, more and more into the individual refraction images of the aperture openings. With circular openings, such as in Figure 2, a system of fine concentric lines appears, while with slit-type openings, such as in Figure 7, a system of parallels between the principal images of the openings occurs. These refraction images also are resolved spectroscopically, and in Figure 5 a refraction image of this type can be seen between the four spectra. The accuracy of the measurement is not influenced in any way by the refraction images, provided the measuring planes are sufficiently distant (for example, a few centimeters) from the focal point. As seen from Equation (8), this distance has no direct influence whatsoever on the accuracy of the result. It should merely not be chosen unnecessarily

large, however, because the brightness of the images always is smaller at greater distances from the focal point.

16. Before the description of the study of the above-mentioned objective is begun as an example, a few words will be said about suitable light sources. The use of the mercury lamp for photographs in monochromatic light has already been mentioned above. This lamp can be suitably used for the determination of some points on the color curve, also. If a large number of points are desired for this curve, then the metal-salt-impregnated carbon rods made by Siemens or Bremer are highly recommended. The author's spectroscopic investigation shows that the red Siemens rods contain strontium, the yellow rods contain potassium and calcium, and the white rods contain barium; the Bremer rods are equivalent to the yellow of Siemens. Wavelengths for the refractable parts of the spectra involved can be taken from the tables of Kayser and Runge. For the optical part, the following approximate data can serve to give a general idea of the appearance of these spectra in weak dispersion.

Siemens red carbon (Sr): The intense yellow band  $\lambda = 578-587$  follows the multiline group  $\lambda = 548-554$  in green, and after a fairly unimpressive band in orange there follow three intense bands in red with a maximum at  $\lambda = 647$ .

Siemens yellow carbon (Ca + K): An intensive green band at  $\lambda = 528-540$ , with a maximum at  $\lambda = 532$  is followed by a narrow group of lines at  $\lambda = 559$ , several lines in orange at  $\lambda = 582$ , and then an intensive band in orange at  $\lambda = 598-606$ , with maximum at  $\lambda = 602$ . There then follows a group of lines in red which ends with a fairly weak band at  $\lambda = 627$ ; three lines at  $\lambda = 643-649$  conclude the spectrum.

Siemens white carbon (Ba): After the bright line  $\lambda = 493$  in blue-green, there follows an intensive green band (actually three bands) with a maximum at  $\lambda = 502$ . Next there appears a bright line in yellow-green  $\lambda = 542$  and double line  $\lambda = 553$ . There follows in orange a group of about 12 lines at  $\lambda = 578$  to  $\lambda = 614$ , and then the weaker bands  $\lambda = 634$  and  $645$  and the bright line in red at  $\lambda = 648$ . Dull lines at  $\lambda = 653$ ,  $659$ , and  $667$  conclude the pattern.

The spark spectra of metals, especially that of cadmium, are very suitable for optical measurements of the color curve. The brightest lines of the cadmium spectrum have the following wavelengths:  $\lambda = 468$ ,  $480$ ,  $508$ ,  $534$ ,  $538$ , and  $644$ . It is also easy to measure the magnesium spectrum with its intensive lines at  $\lambda = 448$ ,  $517$  (b-group),

and 656, as well as the zinc spectrum with the lines  $\lambda = 468, 472,$  and  $481,$  the pair  $\lambda = 491, 492,$  and the strong line in the red at  $\lambda = 636.$  In accordance with the proposal of Lehmann, the electrodes are shaped like two knives set parallel to the sighting line. If the electrodes are brought within about 1 mm of each other, the sparks can be used directly as a punctiform light source at 15 m distance from the objective. If the spark is a shorter distance from the objective or if arc spectra are used, then the apparent diameter of the light source must be limited by a diaphragm. The opening itself can be chosen large enough so that it appears to subtend about 10 to 20 arc seconds seen from the objective. Thus, its diameter is 0.5 to 1 mm at 10 m distance and about 7 mm at 100 mm distance. If a ground glass is placed between the arc and the diaphragm, then punctiform images of equal intensity are always obtained, no matter how far away the light source is. The intensity of these light sources is so great that in monochromatic light photography with a filter and also in spectral resolution with a slit spectrograph, the exposure time is between 0.5 and 10 minutes.

17. The study of the previously mentioned 1-m focal length objective will now be taken up. The following observation series were made:

- 1) Series I. Two extrafocal photographs with the aperture shown in Figure 2 in monochromatic light,  $\lambda = 436;$  distance of the light source from the objective  $O = 87.49$  m.
- 2) Series II. Repetition of the same photographs as a check, at  $O = 18.869$  m.
- 3) Series III. Two photographs of the same aperture for  $\lambda = 579$  at  $O = 18.869$  m.
- 4) Series IV. Two photographs of the color curve with the slit spectrograph for zone  $r = 35.5$  mm, at  $O = 18.869$  m.
- 5) Series V. A number of optical measurements for extrapolation of the color curve into the optical region of the spectrum.

For complete investigation of the objective, the six photographs II, III, and IV would have been sufficient. It required about an hour to obtain them.

Microscopic measurement of the photographs and calculation from Equation (1) directly gives the  $\varphi A_{\lambda}^r$  values, which are compiled in the third column of Tables II and III for Series I and II. The fourth column contains the mean  $A_{\lambda}^r$  values of each zone, free of astigmatism, as described in Section 7, and the fifth column (under g) gives the astigmatic length aberration of the meridional intersection involved and thus the quantity  $\varphi A_{\lambda}^r - A_{\lambda}^r.$

Table II. Series I, Zonal Aberration for  $\lambda = 436 \mu\mu$ ,  
 $O = 87.49 \text{ m}$

r (mm)	$\varphi$ (deg)	$\varphi A_{436}^r$ (mm)	$A_{436}^r$ (mm)	g (mm)	B (mm)	x (mm)	$F_{436}^r$ (mm)
6	45	176.94		-0.10			
	135	177.14	177.04	+0.10	990.89	11.10	979.79
10	0	176.44		+0.13			
	90	176.18	176.31	-0.13	990.16	11.08	979.08
14	45	175.94		-0.02			
	135	175.98	175.96	+0.02	989.81	11.07	978.74
18	0	175.86		+0.06			
	90	175.73	175.80	-0.07	989.65	11.07	978.58
22	45	175.86		-0.02			
	135	175.90	175.88	+0.02	989.73	11.07	978.66
26	0	176.17		+0.09			
	90	175.99	176.08	-0.09	989.93	11.08	978.85
30	22.5	176.56		+0.07			
	67.5	176.41		-0.08			
	112.5	176.39		-0.10			
	157.5	176.59	176.49	+0.10	990.34	11.08	979.26
34	45	176.71		+0.03			
	135	176.65	176.68	-0.03	990.53	11.09	979.44
38	0	176.58		0.00			
	90	176.57	176.58	-0.01	990.43	11.09	979.34

The quantities  $A_{\lambda}^r$  and g are the direct results of each measurement series and correspond to the arbitrarily selected object distance O. To reduce the astigmatic differences g and the zonal differences contained in A to infinite object distance, the differential equation given by Dr. Lehmann<sup>12</sup> can be used. In this case, only the absolute amount of aberrations is obtained. In many cases this suffices. To obtain simultaneously the location of the focus in reference to the scale of the eyepiece draw, the author proposes another method. If B is the image distance, and thus the distance of the image from the second principal point, then rigorously:

$$x = B - F = \frac{B^3}{O + B} \quad (9)$$

Table III. Series II, Zonal Aberration for  $\lambda = 436 \mu\mu$ ,  
 $O = 18.869 \text{ m}$

r (mm)	$\phi$ (deg)	$\phi A_{436}^r$ (mm)	$A_{436}^r$ (mm)	g (mm)	B (mm)	x (mm)	$F_{436}^r$ (mm)
6	45	219.82		-0.38			
	135	219.59	219.20	+0.39	1033.05	53.62	979.43
10	0	219.09		+0.25			
	90	218.59	218.84	-0.25	1032.69	53.59	979.10
14	45	218.51		+0.03			
	135	218.46	218.48	-0.02	1032.33	53.55	978.78
18	0	218.33		+0.03			
	90	218.28	218.30	-0.02	1032.15	53.53	978.62
22	45	218.49		+0.01			
	135	218.47	218.48	-0.01	1032.33	53.55	978.78
26	0	218.88		+0.19			
	90	218.50	218.69	-0.19	1032.54	53.57	978.97
30	22.5	219.10		+0.10			
	67.5	218.93		-0.07			
	112.5	219.02		+0.02			
	157.5	218.93	219.00	-0.07	1032.85	53.60	979.25
34	45	219.26		+0.04			
	135	219.18	219.22	-0.04	1033.07	53.63	979.44
38	0	219.21		+0.06			
	90	219.09	219.15	-0.06	1033.00	53.61	979.39

The image distance B differs from the reading A on the eyepiece draw in each case only by an additive constant  $A_0$ , which is equal to the distance of the second principal point of the objective from the photographic plate when the eyepiece is set at the reading  $A = 0$ . The determination of this constant  $A_0$  is the task of "focal length measurement," which will be discussed further below. The result of the following investigation will be given here in the interim. For the telescope investigated,

$$A_0 = 813.85 \text{ mm.}$$

Addition of this number to the tabular values for  $A_{436}^r$  gives the B values in the sixth column. For reduction to focus x, Equation (9) is used to calculate a small table which, as long as a given object distance is used, supplies the reduction directly with the argument B. The last column of Tables II and III then directly gives focal length  $F = B - x$ .



18. The F values found from the two completely independent test series I and II (these were half a year apart) will first be used for determination of the accuracy of the observation. The values are given in Table IV along with the error calculation.

Table IV

r (mm)	Series I (mm)	Series II (mm)	v = II - I (mm)	p	p v <sup>2</sup>	F <sub>436</sub> <sup>r</sup> (mm)
6	979.79	979.43	-0.36	0.36	0.0468	979.61
10	979.08	979.10	+0.02	1.00	4	979.09
14	978.74	978.78	+0.04	1.96	31	978.76
18	978.58	978.62	+0.04	3.24	518	978.60
22	978.66	978.78	+0.12	4.84	697	978.72
26	978.85	978.97	+0.12	6.76	973	978.91
30	979.26	979.25	-0.01	9.00	9	979.26
34	979.44	979.44	0.00	11.56	0	979.44
38	979.34	979.39	+0.05	14.44	361	979.36
					0.3061	

The weighted values p are proportional to r<sup>2</sup> because of the dependence of the error on radius r given by Equation (8): the unit chosen is the weight for r = 10 mm, which is thus very close to F/100. There follows from the sum p v<sup>2</sup> = 0.3061:

$$\text{mean error of an A value at } \frac{r}{F} = 100 \quad \pm 0.139 \text{ mm}$$

and, in general,

$$\Delta = \text{mean error of an A value} = \pm 0.00139 \frac{F}{r} \text{ mm.}$$

Here, for example, the mean error of a focus determination is  $\pm 0.037$  mm for the edge zone, which is 1/27,000 of the focal length.

According to Equation (8), the mean error of a measurement of distance e is found from the above values of  $\Delta$  to be:

$$\epsilon = \pm 0.0038 \text{ mm ,}$$

which verifies the data given in Section 14.

19. The last column of Table IV (under  $F_{436}^r$ ) gives the mean values of the two series on which subsequent calculation is based. It should be pointed out that the "focal length" of a zone found in the manner given is the distance of its focal point from the second principal point of the axial ray and thus differs from the "combining distance," which is the distance of the focal point from the apex of the latter surface, by only a constant—the distance of the apex from the principal point. This definition, of course, differs from that common in practical optics, which calculates the distance of the focal point involved from the intersection point with the prolongation of the incident ray, but it is close to the general idea of the concept of "focal length." If the instrumental constant  $A_0 = 813.85$  mm is subtracted from  $F$ , the settings on the eyepiece draw are directly obtained. In addition, the  $F$  values immediately give the curve of the zonal aberration for  $\lambda = 436$ . To indicate the latter clearly, it is only necessary to plot the numbers involved in a rectilinear coordinate system as a function of  $r$ , as has been done in the upper curve of Figure 8. This curve simultaneously gives the curve for zonal aberration, as well as the true focal lengths for light of wavelength  $\lambda = 436$ .

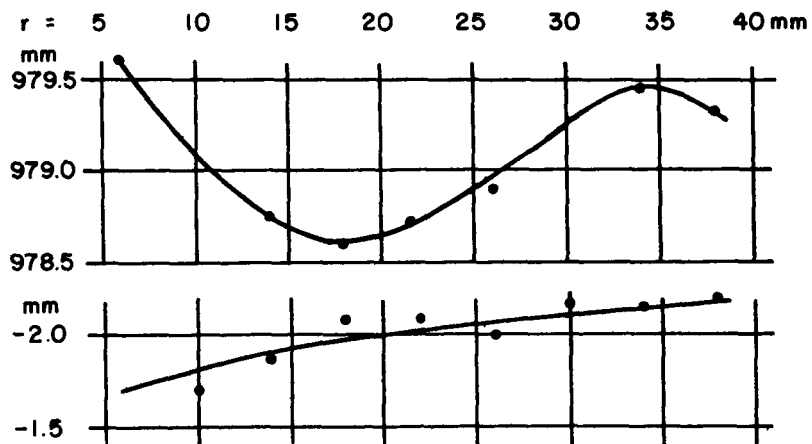


Figure 8. Upper Curve: Focal Length and Zonal Aberration for  $\lambda = 436 \mu\mu$ . Lower Curve: Chromatic Difference  $F_{579} - F_{436}$

20. The reduction of Series III for  $\lambda = 579 \mu\mu$  is done in exactly the same manner. The results alone are given in Table V; the astigmatic differences  $g$  are given in the third column, and the focal length  $F_{579}^r$  values are given in the fourth column. The latter values can now be plotted in the coordinate system of Figure 8, giving a second curve

of zonal aberration which is nearly parallel to the first. It becomes clearer, however, if it is plotted graphically as the difference  $h = F_{579}^r - F_{436}^r$ , which is given in the sixth column. Here it would have to be a constant if the chromatic difference of spherical aberration were to be zero, and the deviation of the  $h$ -curve plotted in Figure 8 from a horizontal line is thus the curve of that difference. Because of the small photographic activity of  $\lambda = 579$  light, the pictures of Series III are somewhat dull and the measurement therefore less certain. In addition, the innermost zone  $r = 6$  could not be measured because of the smaller aperture openings.

Table V. Series III, Zonal Aberration for  $\lambda = 579 \mu\mu$

r (mm)	$\varphi$ (deg)	g (mm)	$F_{579}^r$ (mm)	$F_{436}^r$ (mm)	h (mm)
10	0	+0.05			
	90	-0.05	977.40	979.09	-1.69
14	45	+0.21			
	135	-0.21	976.91	978.76	-1.85
18	0	0			
	90	0	976.53	978.60	-2.07
22	45	+0.01			
	135	-0.01	976.64	978.72	-2.08
26	0	+0.08			
	90	-0.09	976.91	978.91	-2.00
30	22.5	+0.11			
	67.5	-0.08			
	112.5	-0.09			
	157.5	+0.07	977.11	979.26	-2.15
34	45	+0.09			
	135	-0.09	977.30	979.44	-2.14
38	0	-0.10			
	90	+0.09	977.12	979.36	-2.24

Because each A value differs from the corresponding F value by merely a constant, the differences of the corresponding F values can be substituted directly into Equations (4) and (5) for the differences of two A values. With  $\lambda_1 = 436 \mu\mu$  and  $\lambda_2 = 579 \mu\mu$  substituted into Equation (4),  $A_{\lambda_2}^r - A_{\lambda_1}^r = h$ .

21. The g values from the three series will now be compiled for a study of astigmatism. Since these series are based on finite object

distance O, they must first be reduced to infinity, which can be done for these small quantities by the simple equation:

$$dF = dB - \frac{2B}{O} dB .$$

For Series I,  $2B/O = 1/44$ , and thus the reduction is very small; for Series II and III,  $2B/O = 1/9$ . In this manner, the numbers based on position angle  $\phi$  in Table VI are obtained. Although these exceed the inaccuracy of measurement by only a small amount, the same dependence of sign on position angle is nevertheless evident in all the series. This is even more clearly shown if the g values are written at points indicated by coordinates r and  $\phi$  in a circle which represents the aperture of the objective. This has been done in Figure 9, and the positive values have been circled to emphasize them; this gives the absolute amount and the location of the astigmatism at a glance. If there is considerable astigmatism, then the constants a and  $\phi_0$  of Equation (2) can be calculated from the g values. In the case at hand, it is less than 0.1 mm.

Table VI. Astigmatism

$\phi$ (deg)	r (mm)	Series I (mm)	Series II (mm)	Series III (mm)	g (mm)
0	10	+ 0.13	+ 0.22	+ 0.04	+ 0.13
	18	+ 6	+ 3	0	+ 3
	26	+ 9	+17	+ 7	+11
	38	0	+ 5	- 9	- 1
22.5	30	+ 7	+ 9	+10	+ 9
45	6	-10	-34	-	(-22)
	14	- 2	+ 3	+19	+ 7
	22	- 2	+ 1	+ 1	0
	34	+ 3	+ 4	+ 8	+ 5
67.5	30	- 8	- 6	- 7	- 7
	90	10	-13	- 4	-13
90	18	- 7	- 2	0	- 3
	26	- 9	-17	- 8	-11
	38	- 1	- 5	+ 8	+ 1
	112.5	30	-10	+ 2	- 8
135	6	+10	+35	-	(+22)
	14	+ 2	- 2	-19	- 6
	22	+ 2	- 1	- 1	0
	34	- 3	- 4	- 8	- 5
157.5	30	+10	- 6	+ 6	+ 3

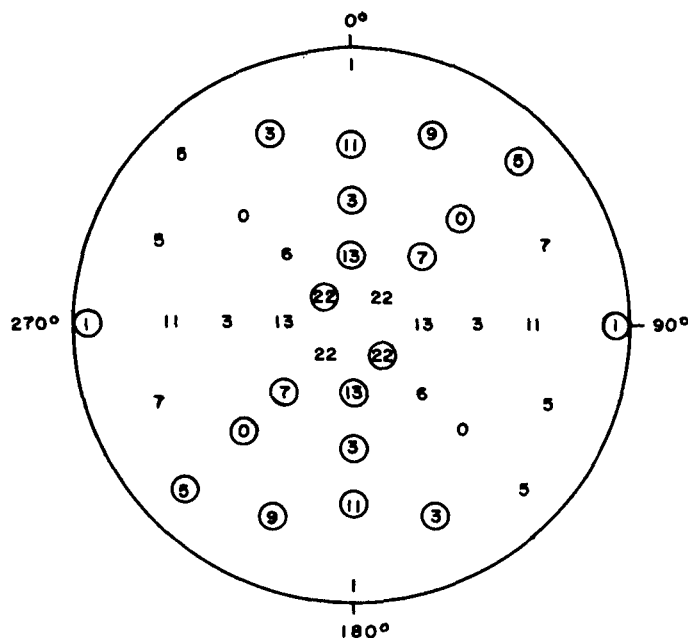


Figure 9

22. The two photographs taken with the spectrograph, as well as the measurement with the eyepiece spectroscope for extrapolation of the color curve to the optical spectrum, were made at only the position angle  $\varphi = 90$  degrees and for the zone  $r = 35.5$  mm. As Figure 9 shows, however, astigmatism is nearly zero for these points, so that astigmatism may be ignored. Reduction of the measurements shows nothing new; therefore, the results will be given directly.

The spectroscope, with the yellow Siemens carbons as a light source in the arc lamp, was used to determine the four values:

Series IV	$\lambda$ ( $\mu\mu$ )	$F_{\lambda}^{35.5}$ (mm)
	393	983.02
	423	980.11
	455	978.48
	488	977.70

In addition, optical measurements using the cadmium spark gave:

Series V	$\lambda$ ( $\mu\mu$ )	$F_{\lambda}^{35.5}$ (mm)
	480	977.84
	508	977.36
	536	977.18
	644	977.43

and with sodium light used: 589 977.22.

These nine observations were used to plot the color curve shown in Figure 10.

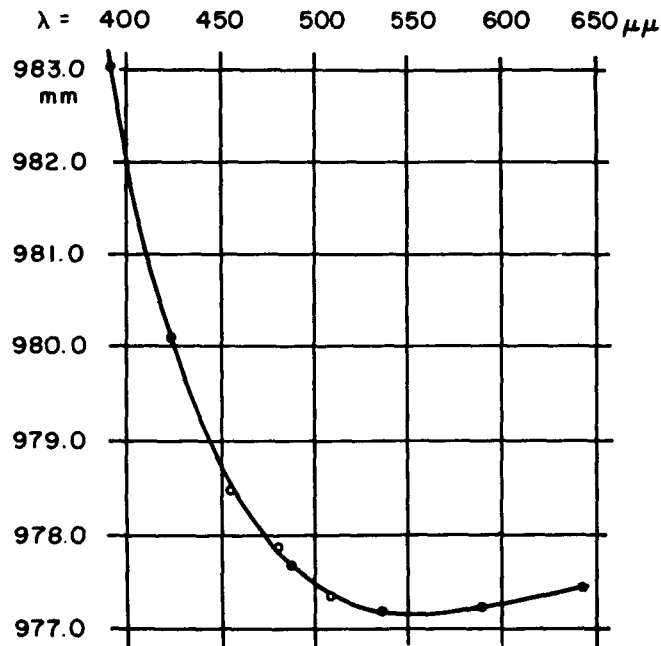


Figure 10. Color Curve. Focal Lengths of Zone  $r = 35.5$  mm

Here, too, the accuracy with which the individually observed points can be represented by a curve gives an indication of the reliability of the measurement. Comparison with the focal-length curve in Figure 8 gives a further check. If the focal length for  $r = 35.5$  mm is read from the latter curve, there is obtained  $F_{436}^{35.5} = 979.43$  mm, and from Figure 10 for  $\lambda = 436$  there is obtained  $F_{436}^{35.5} = 979.39$  mm. In view of the entirely different methods by which these two values were found, the agreement is extremely satisfactory.

23. The four graphic representations in Figures 8, 9, and 10 completely determine all the properties of the axial image; therefore, these three figures, as the simplest and most readily understandable form, are considered to summarize the results of an exact objective study.

A second related form, which consists of tabulation of the values from Figure 8 as a function of  $r$  and those of Figure 10 as a function of  $\lambda$ , will merely be mentioned.

It was of greater interest to calculate, on the basis of the data given in Figures 8 and 10, the focal lengths for a fairly large number of zones and wavelengths by Equation (4), because this gives a clear idea of the three-dimensional configuration of all the focal points. I have summarized the results of this calculation in Table VII, with the first figures of the  $F$  values omitted in all cases. Heavier separating lines were drawn at the places where  $F$  reached the values 977.00 and 978.00. It is immediately seen from this table that nearly all the optically significant light is joined within the 1-mm distance from 976.62 to 977.6. It then became of interest to determine at what point in this distance focusing is done when white light is used with the full aperture. A series of settings to "sharp image" gave an average  $F$  of  $977.2 \pm 0.15$  mm, and this value is fully corroborated in Table VII when it is recalled that the focus of the external zones is decisive. It is easily seen that in this objective a reduction of zonal aberration would contribute very little to improvement of the image if at the same time the secondary spectrum were not reduced.

24. As has already been mentioned, in many cases with telescope objectives the investigation can be simplified if the spherical difference of chromatic aberration is neglected. It is most advisable, then, to determine the zonal aberration for the inflection point of the color curves, and thus  $\lambda = 550$  in the case at hand, and to determine the color curve for a zone near the objective edge, preferable at an inflection point of the zonal aberration curve, and thus approximately at  $r = 34$  mm.

If it is not desired to derive definitive numerical values but merely to obtain a quick idea of the curve of zonal aberration, then the method can be employed in another form. If the two inner slits in the aperture of Figure 7 are extended to the edge of the objective (the two outermost can be omitted), then in the extrafocal position of the measuring plane these two slits are seen as straight lines only when the zonal aberration is zero. The curvature of the lines thus allows a conclusion on the type of zonal aberration without measurement, merely by looking into the

Table VII

$\lambda =$	400	420	440	460	480	500	520	540	560	580	600	620	640	660
$r = 6$	81.74	80.33	79.46	78.81	78.41	78.11	77.96	77.88	77.88	77.91	77.95	78.00	78.07	78.17
8	81.52	80.07	79.16	78.19	78.08	77.77	77.61	77.53	77.53	77.56	77.60	77.66	77.73	77.83
10	81.36	79.86	78.93	78.24	77.81	77.50	77.33	77.25	77.25	77.28	77.32	77.38	77.45	77.56
12	81.22	79.68	78.74	78.03	77.59	77.27	77.10	77.02	77.02	77.05	77.09	77.15	77.23	77.33
14	81.13	79.56	78.59	77.87	77.43	77.10	76.93	76.84	76.84	76.87	76.91	76.98	77.06	77.17
16	81.05	79.46	78.48	77.75	77.29	76.96	76.79	76.70	76.70	76.73	76.77	76.84	76.92	77.03
18	81.04	79.43	78.43	77.68	77.22	76.89	76.71	76.62	76.62	76.65	76.70	76.76	76.84	76.95
20	81.13	79.49	78.48	77.72	77.25	76.91	76.73	76.64	76.64	76.67	76.72	76.78	76.86	76.97
22	81.24	79.57	78.54	77.78	77.30	76.96	76.78	76.69	76.69	76.72	76.77	76.82	76.90	77.01
24	81.35	79.67	78.63	77.86	77.36	77.02	76.84	76.76	76.76	76.79	76.84	76.89	76.97	77.08
26	81.52	79.81	78.76	77.97	77.48	77.13	76.94	76.85	76.85	76.88	76.93	77.00	77.08	77.20
28	81.71	79.99	78.93	78.13	77.64	77.29	77.10	77.00	77.00	77.03	77.07	77.14	77.22	77.34
30	81.89	80.15	79.07	78.27	77.77	77.43	77.24	77.14	77.14	77.17	77.21	77.28	77.36	77.48
32	82.02	80.27	79.18	78.37	77.87	77.51	77.31	77.22	77.22	77.25	77.30	77.37	77.46	77.57
34	82.12	80.35	79.25	78.43	77.93	77.57	77.37	77.28	77.28	77.30	77.35	77.42	77.51	77.62
36	82.11	80.33	79.23	78.41	77.90	77.53	77.33	77.24	77.24	77.27	77.32	77.39	77.48	77.60
38	82.04	80.24	79.13	78.30	77.78	77.41	77.21	77.12	77.12	77.15	77.20	77.27	77.36	77.48
40	81.92	80.11	79.00	78.16	77.65	77.27	77.07	76.98	76.98	77.01	77.06	77.13	77.22	77.34



eyepiece. This method can be used only for fairly long focal lengths, however, at which the aberrations are sufficiently large linearly. The optician should find this shortcut method useful for continuous check of his work.

Another method, proposed for this purpose by Dr. Lehmann, consists of stereoscopic comparison of photographs taken before and behind the focus. The images must be equal in size and require a large number of aperture openings on one diameter.

However, in particular cases the investigation must be done more thoroughly. If some values of the astigmatic differences indicated above by  $g$  show large deviations, then it may be concluded that the objective has local nonuniformities exactly behind the aperture openings involved; then the measurement must be extended to other points of the zone. Local defects of this type are most readily seen when the circular aperture mentioned in Section 11, which leaves open the entire zone between radius  $r$  and  $r + \varrho$ , is used to make an extrafocal photograph. If astigmatism is present, then this aperture ring images as an ellipse; an image of this ellipse can then be used instead of the diagram of Figure 9.

If the objective is investigated in the laboratory, as was done here, the temperature can be held within close tolerances. The astronomer, who must subject his objectives to greatly varying temperatures in the study of it, must remember that both the form of the aberration curve, and especially the focal length, are functions of temperature. He can determine the temperature coefficients of  $A$  and  $F$  very closely through the extrafocal measurements. For the measurement of zonal aberration, the days chosen should be ones in which the objective is not subjected to severe temperature variations, because if different parts of the objective are heated unequally the curve of zonal aberration will be substantially changed.

## B. DETERMINATION OF FOCAL LENGTH

25. According to the Gaussian theory, the focal length of a lens system is defined as the distance of its focal point from the second principal point. If  $AB$  is a ray incident parallel to the axis and  $EL$  is the path of the refracted ray (Figure 11), then  $L$  is the focal point, and the principal point  $P$  is obtained by dropping the perpendicular  $CP$  to the axis from the intersection point  $C$  of the prolonged rays  $AB$  and  $EL$ . Accordingly,  $PL = G$  is the focal length. If the height of incidence  $CP$

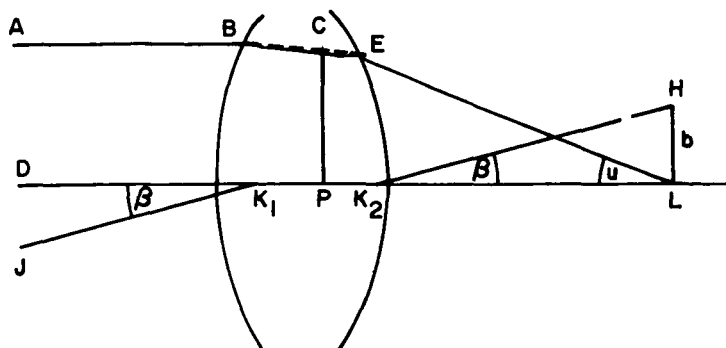


Figure 11

is designated by  $r$  and the angle which the refracted ray makes with the axis is designated by  $u$ , then the Gaussian definition of focal length is:

$$G = \frac{r}{\tan u} \quad (10)$$

A method for determining  $G$  can be based directly on this defining equation if the corresponding values of  $r$  and  $u$  are measured; Féry<sup>13</sup> has recently described an instrument for making these measurements. I shall mention only in passing that if the light source is at an infinite distance, the previously described extrafocal measurements would give the focal length directly from Equation (1), provided the distance  $r$  of the aperture openings from the axis is determined precisely. Through use of the earlier notation, there is obtained:

$$\tan u = \frac{e_1 + e_2}{2(A_2 - A_1)},$$

and consequently

$$G = \frac{2r(A_2 - A_1)}{e_1 + e_2} \quad (11)$$

This method is certainly not to be recommended, however.

In the Gauss-Abbe theory, which (beginning with a pointwise imaging by straight rays) gives in rigorous mathematical form the general relationships between the object space and the image space, Equation (10) is generally valid. That is, all incident rays parallel to the axis converge after refraction in such manner that they intersect at a single focal point  $L$ ; and, in addition, the intersection points  $C$  all lie in the same plane  $CP$ , the second principal plane of the system. In this case, the focal length  $G = PL$  is uniquely defined, also.

However, in actual dioptric systems the relationships are entirely different. It was shown above that since focal point  $L$  does not have a fixed position, it can differ by several millimeters for the various rays. The second terminal point of the ray  $PL$ , the base  $P$  of the perpendicular  $CP$ , is also afflicted with aberrations in the same manner. The simple plano-convex lens gives a very clear demonstration of this. Any axially parallel ray  $AB$  incident from the planar side of the lens (Figure 12) reaches the spherical surface unrefracted. In consequence, in this case the intersections  $C$  of the incident and the refracted ray coincide on the spherical lens surface. The location of the base  $P$  is therefore a function of the height of incidence  $r$ , and if  $r = 0$ , then  $P$  in this case reaches the lens apex  $P'$ . Depending upon the form of the lens system, point  $P$  can depend in a different manner upon the height of incidence; but for infinitely small values of  $r$ ,  $P$  will approach a limiting position  $P'$ , which is designated as the second principal point of the system. The distance of focal point  $L$  of the rays near the axis (the null rays, as they are called) from this second principal point is then called the principal focal length of the system.

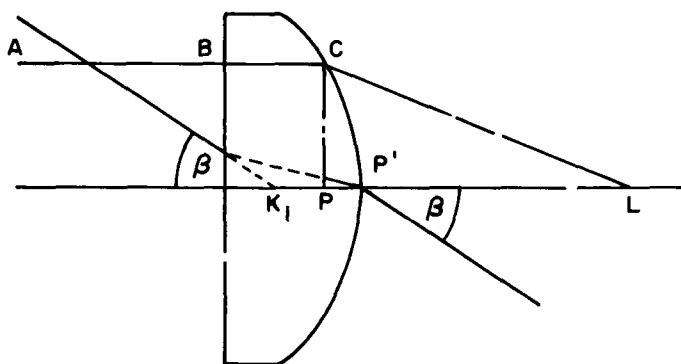


Figure 12

The focal length of incident ray  $AB$ , parallel but at a considerable distance from this axis (Figure 11), is customarily understood in present optical practice to be not the Gaussian length  $PL$  but rather the length  $CL$ ; and  $C$  is also called the principal point of the ray  $AB$ . To avoid any confusion here, I shall designate  $P$  as the axial,  $C$  as the lateral principal point, and  $CL = S$  as the lateral focal length. The designation of the distance  $CL$  as the focal length of the lateral ray is based on the similarity of the role played by this distance to that of the principal focal length for the null rays. If spherical aberration is eliminated along the axis in the system, and if this is also done for points away from the axis, so that the system is aplanatic, then the sine

condition is necessarily fulfilled, so that in telescope objectives the further condition  $CL = \text{constant}$  for all zones of the objective results. In this case, the lateral principal points  $C$  lie on a sphere described around the focal point  $L$  with a radius  $CL$  which is identical with the principal focal length.

26. For the practical observer, the last-mentioned concept of focal length is of little practical use. The observer always connects the term "focal length" with another and completely fixed concept, namely, the ratio of the linear size of the image of an infinitely distant object to its apparent size. If  $\beta$  (Figure 11) is the apparent size of an infinitely distant object (for example, the sun) and  $b = HL$  is the size of the image appearing in the focal plane, then the focal length  $K_2L = F$  is defined by:

$$F = \frac{b}{\tan \beta} \quad . \quad (12)$$

Gauss<sup>14</sup> also gives this definition and says that it may be "in reality" the only suitable one.

According to this definition, the focal length is the distance of the focal point from the second nodal point  $K_2$  of the system. If  $K_2$  is at the same location for all values of  $\beta$ , then  $F$  is constant for all image sizes; therefore, the system is free of distortion (assuming that an extensive sharp image is produced in the focal plane). The plano-convex lens (Figure 12) again is an example of this type of stable position of the second nodal point. In this lens, it always coincides with the apex point  $P'$  for any value of  $\beta$ , while the location of the first nodal point is a function of  $\beta$ . In general, the position of  $K_2$  varies with  $\beta$ .  $K_2$  approaches a fixed limiting position as  $\beta$  decreases, and this position coincides with the above-mentioned limit position of  $P$  (that is, with the second principal point of the system). In this latter case, where the system has distortion, the ratio  $b/\tan \beta = F$  in Equation (12) is not a constant but instead approaches a limiting value as  $\beta$  decreases; and the limiting value is seen to be identical with the principal focal length: it is the distance of the focal point from the second principal point of the system.

The absolute value of the height of incidence  $r = CP$  no longer enters this last definition of focal length. In other words, the focal length is understood for any outer zone of the objective to be merely the distance of its focal point from the above-defined second principal point of the system and thus neither from the movable point  $P$  nor from

the lateral principal point C. The focal length  $F$  thus defined is differentiated from the combining distance (which, as is well known, is calculated from the apex of the lens) only by a constant, which is the distance of the lens apex from the principal point. On the other hand, the focal lengths of the various zones of the objective differ from each other merely by the amount of spherical aberration. I have not presented any new definition of focal length here but have sought merely to express as clearly as possible the idea which is generally connected with the concept of focal length, because considerable uncertainty on this prevails in many quarters. Thus, for example, it is seen that the above-mentioned method of Féry does not give the focal length from the equation  $G = r/\tan u$ , but the quantity  $G = PL$ , which is in general variable. It would be much more nearly correct to calculate the lateral focal length from the equation  $S = r/\sin u$ .

27. The determination of the importance of  $F$  seen in the previous section makes it possible to determine focal length in an entirely precise manner. The position of the focal points  $L$  of all individual rays in reference to the readings  $A$  at the eyepiece adjustment were determined by the earlier described extrafocal measurements. According to the above, to obtain the focal lengths of all these rays it is only necessary to determine a single constant  $A_0$ , which equals the distance of the micrometer plane from the second principal point at the setting  $A = 0$ . There results in general:

$$F = A + A_0 . \tag{13}$$

This completely separates the task of determination of focal lengths from the study of sharp image location, and it reduces to the determination of the location of the second principal point or nodal point.

Up to the present, there have been no exact experimental investigations of the position of the nodal and principal points. All previous investigations have tacitly assumed that every system has two fixed (that is, aberration-free) principal points the position of which is found in each case by the usual focal-length determinations. I may mention the discussion of Schell, "Determination of the Optical Constants of a Centered Spherical System by Precision Focometer,"<sup>15</sup> as an example of a very thorough paper based on this viewpoint. The usual methods of focal-length determination by sharp focusing on the image at various object distances were so inexact that the small aberrations of the principal points could scarcely be determined thereby. I shall describe further below a new, exact method for measurement of the location of the principal points.

The aberration of the second nodal point (that is, as a function of  $\beta$ ) can easily be studied on the basis of Equation (12); every measurement of distortion also is a determination of this aberration. In astronomical objectives, the field of view of which is used only in the vicinity of the axis, it is generally unnoticeable. On the other hand, it can attain significant amounts in photographic lenses, and I shall discuss this later in greater detail.

28. I have proposed three different methods for determination of the constant  $A_0$  for the previously described telescope objective. The first and the second of these are based on determination of the second nodal point, and the third is based on observation of the location of the principal point.

The nodal point is determined by means of the observation method traditionally used in astronomy; it consists of the above-mentioned measurement of the image size of an object of known angular extension. The method possesses the advantage—hitherto generally unnoticed—of being completely independent of proper focusing on the sharp image, because it is possible, as long as measuring accuracy does not suffer, to choose focusing  $A$  arbitrarily and still obtain the same  $A_0$  value. The reason for this is that Equation (12), which can generally be written in the form:

$$B = \frac{b}{\tan \beta} \quad (14)$$

or also as:

$$B = \frac{Ob}{D} \quad , \quad (15)$$

in which the image distance  $B$  is the distance of the measuring plane from the second nodal point,  $D$  is the linear size, and  $O$  the distance of the object from the first nodal point, is merely the expression for perspective imaging of  $K_2$ . Thus, it has nothing to do with the lens' ability to form a sharp image. The only disadvantage of this method is that with telescope objectives  $b$  is always small compared with  $B$ , so that any error encountered in the measurement of  $b$  is greatly magnified in  $B$ . As the following measurements show, it is not easy to determine focal length in this manner more closely than about one thousandth of its value. An accuracy of one part in 10,000 in focal length is achieved only in direct sky observation with large refractors.

Series I. A length  $D = 299.88$  mm was found at a distance of 87.67 m from the telescope. In the setting of the eyepiece adjustment,  $A = 174.51$ , four measurements were made with a filar micrometer, giving as a mean,  $b = 3.382$  mm. In consequence of Equation (15):

$$B = 988.72 \text{ mm}$$

$$A = 174.51 \text{ mm}$$

---


$$A_0 = 814.21 \text{ mm (four measurements).}$$

Since only short distances can be measured with a filar micrometer, the error of  $b$  in  $B$  was magnified 300 times here. In the subsequent photographic measurements,  $D$  was chosen considerably smaller to permit the measurement of the distances  $D$  and  $b$  with the same screw of the measuring microscope.

Series II. Four small openings were made in a small sheet. Six different distances could be measured between them; the mean of the six distances gave  $D = 28.154$  mm. The sheet was illuminated from the reverse side and set at a distance of 18.67 m. Two photographs made at  $A = 216.0$  and  $A = 218.0$  gave  $b = 1.5534$  and  $b = 1.5553$  mm. From Equation (15) there is obtained:

$$B = 1030.1 \text{ mm} \quad 1031.4 \text{ mm}$$

$$A = 216.0 \text{ mm} \quad 218.0 \text{ mm}$$

---


$$A_0 = 814.1 \text{ mm} \quad 813.4 \text{ mm}$$

$$\text{As an Average: } A_0 = 813.75 \text{ mm (12 measurements).}$$

Series III. One of the previous analogous measurement series at a somewhat different  $O$  value and three different  $A$  values gave the values:

$$A_0 = 813.99 \text{ mm}$$

$$814.44 \text{ mm}$$

$$813.50 \text{ mm}$$

---


$$\text{As an Average: } A_0 = 813.98 \text{ mm (18 measurements).}$$

29. Because of the small value of  $b$ , each of the errors in the measurement of this distance in Series II and III enters  $A_0$  magnified 700 times. If these short lengths are to be measured with certitude to 0.001 mm, then  $A_0$  would still be uncertain to several tenths of a millimeter. If  $b$  is chosen considerably larger, then it becomes difficult to measure  $D$  and  $O$  with sufficient sharpness. All these difficulties are

completely eliminated by the following method, which I consider the most reliable for the determination of the second nodal point. An accurately determinable length is placed in the measuring plane of the telescope. I have made one of these by engraving two parallel lines on an exposed photographic plate which was then placed in the cassette and illuminated from the reverse side. The distance  $b$  between these lines is accurately determined under the microscope. Some variety of angular measuring instrument is then placed before the objective of the horizontal telescope and the values of  $\beta$  are measured directly. The method of observing is thus similar to that used in the familiar Gaussian method for determination of the micrometer interval of a telescope focused at infinity.

In Figure 13,  $K_1$  and  $K_2$  are again the nodal points, and  $HL = b$  is the distance in the measuring plane. If, to facilitate matters,  $B$  is chosen smaller than  $F$ , then the objective creates a virtual image of  $b$  on the same side;  $H'L' = D$  will be assumed here. The axis of the angular measuring instrument will be assumed at  $W$ , distant  $K_1W = E$  from the first nodal point. The angle  $\gamma = H'WL'$  is measured instead of  $\beta$ .

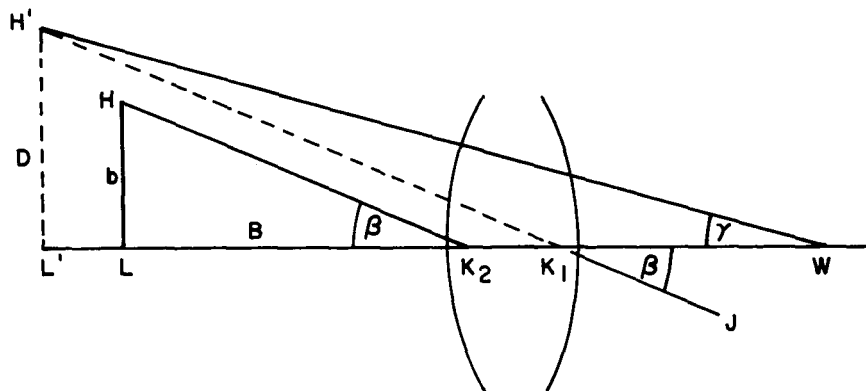


Figure 13

If  $K_1L' = O$  and  $K_2L = B$ , and if  $L'W = Z$  is further assumed, then

$$O = \frac{FB}{F - B}$$

$$Z = O + E = \frac{FB + E(F - B)}{F - B}$$



$$\tan \gamma = \frac{D}{Z} .$$

Since

$$D = \frac{bO}{B} = \frac{bF}{F - B} ,$$

there is immediately obtained

$$\tan \gamma = \frac{b}{B + \frac{E}{F}(F - B)} .$$

If, as before,  $A$  is the reading at the eyepiece adjustment corresponding to image distance  $B$  and if the setting at infinity corresponding to  $F$  is called  $A_{\infty}$  as a differentiation, then

$$F - B = A_{\infty} - A ,$$

and the result is

$$B = \frac{b}{\tan \gamma} + \frac{E}{F}(A - A_{\infty}) . \quad (16)$$

If this expression is compared with Equation (14), it is seen that because of the centering error of the angular measuring instrument the correction term  $(A - A_{\infty})E/F$  occurs. To keep this term as small as possible, the distance to be measured is brought to the neighborhood of the focal point so that  $A - A_{\infty}$  becomes small, or else the measuring instrument must be placed so that its axis passes as closely as possible to the first nodal point  $K_1$ . Spectrometers are thus particularly suitable for these measurements. If the measurements are made symmetrical to  $A_{\infty}$ , so that the factor  $A - A_{\infty}$  is partly positive and partly negative, then a small imprecision in the determination of  $E$  is entirely harmless.

30. For the angular measurements in the method developed above, I have used a spectrometer the circle of which allows 0.1 seconds to be read by means of two microscopes. Table VIII gives the complete calculation of test series IV, in which the axis of the spectrometer passes as accurately as possible through the first nodal point. To show that the result is independent of the setting  $A$ , I varied the latter by as much as 110 mm. In spite of this, the calculated values of  $A_0$  are completely constant even without taking into account the correction term. The distance  $2b$  was 27.482 mm.

Table VIII

A (mm)	$2\gamma$	$\log \tan \gamma$	B (mm)	$A_0$ (mm)
110	1° 42' 16.4"	8.17249	923.7	813.70
160	1° 37' 1.2"	8.14959	973.7	813.71
161	1° 36' 55.7"	8.14918	974.6	813.63
162	1° 36' 47.3"	8.14855	976.0	814.05
163	1° 36' 42.8"	8.14821	976.8	813.81
164	1° 36' 36.6"	8.14774	977.8	813.87
165	1° 36' 30.5"	8.14729	978.8	813.88
166	1° 36' 24.5"	8.14684	979.90	813.90
167	1° 36' 19.5"	8.14646	980.75	813.75
168	1° 36' 13.1"	8.14598	981.84	813.84
220	1° 31' 24.3"	8.12369	1033.55	813.55
Series IV, Mean (11 Measurements): $A_0 = 813.79$				

As an example of a test series made without all the precautions (E and  $A - A_\infty$  very large), Series V, calculated in Table IX, is given here. Here again,  $2b = 27.482$  mm, and the axis of the spectrometer was about 18 cm from the objective.

Table IX

A (mm)	$2\gamma$	$\frac{b}{\tan \gamma}$ (mm)	$\frac{b}{\tan \gamma} - A$ (mm)	$\frac{E}{F}(A - A_\infty)$ (mm)	$A_0$ (mm)
90	1° 42' 55.6"	917.85	827.85	- 13.63	814.22
140	1° 38' 35.2"	958.25	818.25	- 4.35	813.90
161	1° 36' 50.2"	975.57	814.57	- 0.45	814.12
162	1° 36' 42.7"	976.83	814.83	- 0.26	814.57
163	1° 36' 41.2"	977.08	814.08	- 0.07	814.01
164	1° 36' 37.2"	977.75	813.75	+ 0.11	813.86
174	1° 35' 48.3"	986.08	812.08	+ 1.97	814.05
210	1° 32' 59.1"	1015.97	805.97	+ 8.65	814.62
300	1° 26' 45.7"	1088.85	788.85	+25.37	814.22
Series V, Mean (Nine Measurements): $A_0 = 814.17$					

The values given in the fourth column,

$$\frac{b}{\tan \gamma} - A = A_0 + \frac{E}{F}(A - A_\infty) ,$$

in this case show a strong trend which corresponds closely to the term  $(A - A_\infty)E/F$ . Since  $E$  cannot be measured accurately because of the initially unknown position of the first nodal point, the value of the coefficient  $E/F$  is found from the two extreme measurements. This gives

$$\frac{E}{F} = \frac{39.00}{210.0} = 0.1857 .$$

From Section 23,  $A_\infty = 977.2 - 813.8 = 163.4$ , and from this are determined the corrections given in the fifth column. As the last column shows, this correction brings the  $A_0$  values into complete agreement and gives the correct mean value.

A sixth test series, made exactly as was Series IV, gave from 11 observations  $A_0 = 813.58$  mm.

I shall compare the values found from the two methods for nodal-point determination to derive the simple mean from them.

Series I	$A_0 =$	814.21 mm	(4)
II		813.75 mm	(12)
III		813.98 mm	(18)
First Method:	$A_0 =$	813.98 mm	
Series IV	$A_0 =$	813.79 mm	(11)
V		814.17 mm	(9)
VI		813.58 mm	(11)
Second Method:	$A_0 =$	813.85 mm	

31. As this summary shows, the methods described here are sufficient to determine the value of  $A_0$  to 1 mm (that is, one thousandth of the focal length), although 0.1 mm (that is, one ten-thousandth of the focal length) is scarcely possible even by careful conduct of the observations, as in Series IV. Therefore, I sought a more accurate method and have found one in the following method of direct measurement of the position of the principal points.

A microscope is used to make the measurements. Its stage can be moved perpendicular to the optical axis by a micrometer screw. A glass scale with equidistant graduations is placed on the stage, and on this is placed the objective to be studied, removed from the telescope. The rear edge of its mount is in contact with the divided plane of the glass plate. It is then moved on the latter so that the scale is under a diameter of the objective and so that its graduations are symmetrical pairwise about the objective center.

The true distance of two such symmetrical scale marks is  $TT' = 2r'$  (Figure 14). Because the lines of sight of the microscope AC and A'C' are parallel to axis PL when these two lines are set, they converge, after their passage through the objective, along directions TL and T'L to the focal point L of the pertinent zone of the objective. Therefore, according to Section 25, the prolongation of TL intersects line AC at the lateral principal point C (the same is true for C'), while P is the axial principal point, which becomes the second principal point of the system for null rays. In accordance with the previous notation, the distance PC = r, directly measured by microscope in the test setup described, is the radius of the zone utilized; and PL = G is the focal length according to the Gaussian definition in Equation (10). If the distance PN (and thus the distance of the principal point from the rear plane of the objective mount) is called H, similar triangles CPL and TNL give

$$H = \frac{r - r'}{r} G . \quad (17)$$

Because  $(r - r')/r$  is always a very small fraction, the focal length F may be directly used here for  $G^*$ , and accordingly

$$H = \frac{r - r'}{r} F . \quad (18)$$

It is thus extremely simple to determine the position of the principal points by this method. As to the accuracy of the method, the following should be noted. The error occasioned in the measurement of the small difference  $r - r'$  enters H multiplied by the factor  $F/r$  and is therefore the principal source of error in these measurements. It is

---

\*If a rigorous procedure is to be followed, then the values of G can be calculated from Equation (20), with the true values of H obtained from Equation (17).

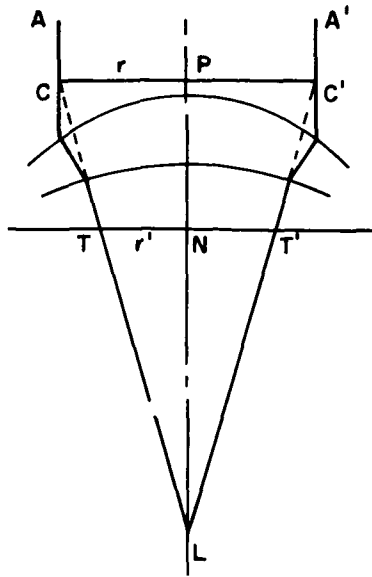


Figure 14

not difficult to reduce the mean error in the measurement of  $r - r'$  to about 0.001 mm; therefore,

$$\text{mean error of } H = \frac{F}{r} 0.001 \text{ mm.}$$

This expression is constructed entirely analogously to the error equation (8) for focal point determination, and it shows that the accuracy with which the principal point of a zone is determined by the method described above is almost exactly the same as that for determination of the focal point through extrafocal measurements under the most favorable conditions.

32. Table X gives the results of the author's measurements by this method.

A photographic plate, on which a grid with 5-mm intervals was photographed, was used as a scale here. Since the measurement gives the values of  $2r$  and  $2r'$  directly and since, in addition, the screw used had a 0.5-mm pitch, the values of  $r$  and  $r'$  given in the table are derived from the screw readings by division by 4. The values given under  $H_I$  are derived from these by Equation (18). Focal length  $F$  was taken from Table VII for  $\lambda = 550 \mu\mu$ , the point of inflection of the color curve and the intensity maximum for optical measurements. If the chromatic aberration of the nodal and principal points, which is important for

Table X. Second Axial Principal Points  
of the Individual Zones

r (mm)	r' (mm)	r - r' (mm)	F (mm)	H <sub>I</sub> (mm)	H <sub>II</sub> (mm)	H (mm)
36.4811	35.0239	1.4572	977.21	39.03	39.02	39.02
31.2761	30.0189	1.2572	977.20	39.28	38.25	39.26
26.0671	25.0151	1.0520	976.85	39.42	39.35	39.38
20.8545	20.0120	0.8425	976.65	39.46	39.43	39.44
15.6419	15.0091	0.6328	976.72	39.51	39.55	39.53
10.4288	10.0059	0.4229	977.19	39.63	39.63	39.63
5.2151	5.0029	0.2122	978.03	39.80	39.78	39.79

objectives to be used for three-color photographs, is sought, then it is only necessary to repeat the measurement at the corresponding monochromatic illuminations. Measurement in white light is adequate for telescope objectives.

The numbers given under H<sub>II</sub> in Table X are the result of a second series of observations made in the same manner on another day after a complete readjustment of the test apparatus. The nearly perfect agreement of the two series indicates the high reliability of the method. The last column (under H) contains the mean of the two series, which I have shown graphically as the first curve of Figure 15 to indicate this "aberration of the second principal point."

For  $r = 0$ , this curve AF gives the position of the principal points of the system as

$$H_0 = 39.93 \text{ mm.}$$

In prolonging the curve through  $r = 5$  mm, it should be noted that it must have a point of inflection at  $r = 0$  and cannot have a peak.

To derive the value of  $A_0$ , that is, the focal length, from the position of the second principal point found here, it is only necessary to measure the tube length of the telescope. This has been done with the aid of a steel bar rounded on the ends, held loosely on the axis of the tube by two diaphragms. The tube was turned vertically, and the bar then rested with its own weight on a glass plate fastened in the cassette. Movement of the eyepiece adjustment then caused the upper end of the bar to touch a rule placed above the upper end of the telescope (after the objective had been removed). The length of the bar was then

accurately determined with two good meter sticks. In this manner, the tube length from the rear edge of the objective mount to the plate plane at setting  $A = 0$  was found to be 773.80 mm. If the value  $H_0 = 39.93$  mm is added to this, there is obtained

$$A_0 = 813.73 \text{ mm.}$$

This result should be accurate to about 0.1 mm; the principal source of its uncertainty is in the extrapolation of  $H$  for  $r = 0$ .

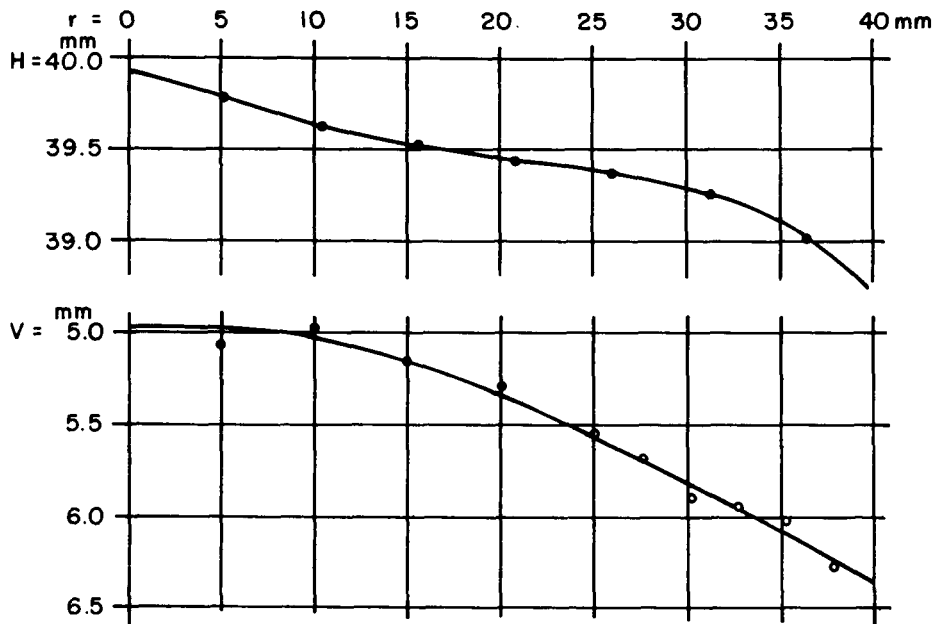


Figure 15

Before this figure (derived from the position of the second principal point) was joined to the earlier values of  $A_0$ , which had been determined with the aid of the property of the second nodal point, it was necessary to note that the two results do not necessarily agree with each other. The limiting positions of the principal and nodal point coincide, but the number derived from the image size in the manner described above will give the true position of the second nodal point only if the image projected by the objective is free from coma, that is, from asymmetrical spherical aberration outside the principal axis. If the objective has coma, then the measurement of image size will give a point of concentration of the image which need not coincide with the point at which the ray through the second nodal point (and thus parallel to the incident direction) strikes the measuring plane.

The objective in this case is, as is seen from the close agreement of the values of  $A_0$  found by the various methods and as could be proven more rigorously, free from coma; therefore, the mean is taken directly from the result of the three methods.

First method for determination of nodal point:	$A_0 = 813.98$ mm
Second method for determination of nodal point:	813.85 mm
Determination of principal point:	813.73 mm
Mean:	$A_0 = 813.85$ mm

This mean value is the number already given in Section 17. It is probably very close to being accurate within 0.1 mm, meaning that the focal length of the objective has been determined within one ten-thousandth part of its value.

33. To find the position of the first principal point, a knowledge of which is frequently necessary for exact measurement of the object distance  $O$ , it is merely necessary to repeat the measurement described in the preceding section, with the objective reversed on the scale plate. Table XI shows the result of a single measurement. In accordance with Equation (18), this gives the distance of the first principal point from the plane of the forward edge of the objective mount, which has been designated by  $V$  to distinguish it from  $H$ . The values of  $V$  are shown in the second curve of Figure 15, from which there is obtained again, by extrapolation to  $r = 0$ , the position of the first principal point of the objective:

$$V_0 = 4.99 \text{ mm.}$$

It is seen from Figure 15, in which the ordinates  $H$  and  $V$  are plotted in opposing directions, that the distance of the two principal points from one another is nearly constant; both approach the rear side of the objective together as  $r$  increases.

The following dimensions will be mentioned in passing:

Distance of the first lens apex from the front mounting edge:	2.4 mm
Distance of the last lens apex from the rear mounting edge:	32.8 mm
Distance of the front mounting edge from the rear mounting edge:	50.1 mm



From this it is found that:

Distance of the first principal point from the first lens apex:	2.6 mm
Distance of the second principal point from the first lens apex:	7.8 mm
Distance of the second principal point from the last lens apex:	7.1 mm
Thickness of the system:	14.9 mm
Distance between the principal points (Interstitium):	5.2 mm

Table XI. First Axial Principal Points of the Individual Zones

r (mm)	r' (mm)	r - r' (mm)	F (mm)	V (mm)
37.7645	37.5232	0.2413	977.14	6.27
35.2410	35.0239	0.2171	977.27	6.02
32.7192	32.5202	0.1990	977.25	5.94
30.2012	30.0189	0.1823	977.15	5.90
27.6775	27.5165	0.1610	976.97	5.68
25.1578	25.0151	0.1427	976.81	5.54
20.1212	20.0120	0.1092	976.63	5.30
15.0890	15.0091	0.0799	976.76	5.17
10.0572	10.0059	0.0513	977.24	4.98
5.0290	5.0029	0.0261	978.07	5.07

### C. FULFILLMENT OF THE SINE CONDITION

34. Determination of the position of the axial principal points now makes it possible to answer the second question of interest, whether the sine condition is fulfilled in the objective under study. If this is the case, then, as mentioned above, the lateral focal length  $S = LC$  (Figure 11) will be a constant. To test whether the condition mentioned is fulfilled, it is merely necessary to calculate the values of  $S$  for the individual zones; the numbers for this can be taken directly from Table X.

$$S = \sqrt{G^2 + r^2}, \quad (19)$$

in which

$$G = F - (H_0 - H). \quad (20)$$

If these equations are used for calculation, the numbers given under S in Table XII are obtained. These values are by no means constant since their extremes differ by 1.52 mm.

Table XII.

r (mm)	H <sub>0</sub> - H (mm)	F (mm)	G (mm)	S (mm)	G' (mm)	S' (mm)	Difference (mm)
36.48	0.91	977.21	976.30	976.98	976.43	977.11	- 0.02
31.28	0.67	977.20	976.53	977.03	976.68	977.18	+ 0.05
26.07	0.55	976.85	976.30	976.65	976.84	977.19	+ 0.06
20.85	0.49	976.65	976.16	976.38	976.88	977.10	- 0.03
15.64	0.40	976.72	976.32	976.45	976.93	977.06	- 0.07
10.43	0.30	977.19	976.89	976.95	977.03	977.08	- 0.05
5.22	0.14	978.03	977.89	977.90	977.16	977.17	+ 0.04
					Mean:	977.13	

Although it may appear here that the sine condition is not fulfilled, it can be easily seen that the differences in S are caused merely by zonal aberration. To show this, the calculation has been repeated under the assumption that F = constant = 977.20 mm. At constant F, Equation (18) gives somewhat different values of H; H<sub>0</sub> = 39.80 mm. Of course, these values are not yet extremely rigorous for the aberration-free objective, because the same cause of the zonal aberrations in F—whether it is an error in the manufacturing of the surfaces or a nonuniformity in the density of the glass—must necessarily give small zonal aberrations in the observed values of r. Of course, the substitution of F = constant largely eliminates the influence of zonal aberration. The values G' and S' in Table XII resulted from this, and it is seen from the deviations from the mean value of S' = 977.13 mm, given in the last column, that the lateral focal lengths S' are constant within the accuracy of measurement. The sine condition is accordingly fulfilled in the objectives studied, and thus the aberration is corrected away from the axis. As soon as the zonal aberrations are eliminated by retouching, the lateral focal lengths S will come into strict agreement.

The mean value of  $S$ , which is no longer harmfully affected by the above-mentioned extrapolation of  $H_0$ , would then necessarily be considered as the true value of the focal length of the objective as a whole. It has an accuracy which is close to 0.01 mm, that is, one hundred-thousandth part of the focal length.

If it were sought to use the objective under consideration in the reverse position, then, as indicated by the parallel path of the curves for  $H$  and  $V$ , the sine law would no longer be fulfilled and a considerable impairment of the images of elongated objects would necessarily be experienced.

35. Following the above description of the methods for measurement of individual errors of a telescope objective, a few words will now be devoted to the requirements which must be made of such an objective.

If the sine requirement is not fulfilled, then even if the spherical aberration were completely corrected, the individual zones of the objective would give images of different size; therefore, poor definition of the images off the axis and asymmetric elongation (coma) would occur for punctiform objects such as stars. Since the sharp definition of the image site is lost thereby, it is necessary to require that the sine condition be fulfilled for all objectives which are to be used for exact measurements in the image plane.

The harmful effect of chromatic aberration depends to a great extent upon the nature of the observed object and in part also on the eye of the observer. It is, therefore, not possible to derive (for example, from the values of all  $F\lambda^{\text{r}}$  given in Table VII) in a generally valid manner a mean value  $F_0$ , which would correspond to the setting for white light with the full aperture used. Of course, as was discussed in Section 23, it is possible to determine an approximate value of  $F_0$  by direct observation, but even when this value is known, it is still not possible to calculate satisfactorily the size and intensity of the image disks appearing in the image plane and corresponding to  $F_0$ . The rules of geometric optics fail in this case. Here it is important to synthesize the effect of the entire objective from the effect of its individual zones, and only theoretical refraction studies<sup>6,16</sup> can lead to the goal here. Since these investigations lead to such laborious calculations as to prevent their general application, it is necessary to propose a more convenient even though less rigorous way. Since the theoretical refractive requirement that the light wave after its passage through the objective have the shape of a spherical wave is identical with the geometric requirement that all rays intersect at one point,

the size of the purely geometrically calculated image disks can doubtless serve as a measure of the degree to which the above requirement of refraction theory is fulfilled. The values thus determined geometrically have nothing to do with the actual diameter of the image disks in the setting plane; however, in fact the case can frequently occur in which the smallest or sharpest and brightest interference image does not even lie in the setting plane which geometrically corresponds to the smallest disk.

Matters are entirely different as far as the effects of chromatic aberration are involved. Since rays of different wavelengths are not able to interfere, the intensities of all the individual wavelengths merely add to form corresponding diffraction images, and the diameter of the total image in any setting plane is determined by the greatest monochromatic diffraction image in this plane. If the objective for the part of the spectrum involved is not sufficiently achromatic, then the smallest diffraction disk corresponding to any single color can no longer be observed, because at the plane in question there are always larger disks of other colors. This shows how important it is to make the color corrections as completely as possible, entirely aside from the possible amounts of zonal aberration, or, if the object is sufficiently bright, to cut out the disturbing parts of the spectrum by using a ray filter chosen on the basis of the color curves.

36. To obtain a simple and reliable measure of the quality of the objective as the geometrically calculated size of monochromatic diffusion circles, calculation is made in the following manner. It is best to do the calculation for that wavelength which corresponds to the point of inflection of the color curve. The zonal aberration is known for this wavelength from Section 24; for the objectives under consideration, they are the figures of Table VII in the column  $\lambda = 560 \mu\mu$ .

The value  $F_0$ , which corresponds to the smallest geometric circle, is first determined. For this purpose, the maxima and minima closest to the edge are read off the curve of zonal aberration. In this case, these are:

$$r_1 = 34 \quad F_1 = 977.28$$

$$r_2 = 18 \quad F_2 = 976.62.$$

The smallest image diameter appears when the circles produced by these two zones are of equal size. This gives the requirement

$$(F_1 - F_0) r_1 = (F_0 - F_2) r_2,$$

from which there is obtained

$$F_0 = \frac{F_1 r_1 + F_2 r_2}{r_1 + r_2} .$$

(To facilitate calculation, a constant—about 976—can be subtracted from all  $F$  values.) From the above figures,  $F_0$  is found to be 977.05.

In the plane corresponding to the value  $F_0$ , there is then obtained the diameter  $d$  of the diffusion circles of all zones from

$$d = 2 r \frac{F - F_0}{F_0} , \tag{21}$$

and the maximum of the  $d$  value thus calculated will correspond to the above extremes  $F_1$  and  $F_2$ . If the latter is not the case, but instead a larger  $d$  results for some zone  $r_3$ , then  $F_0$  must be recalculated with  $r_3$  and  $r_1$  or with  $r_3$  and  $r_2$ . This case occurs in the example here; instead of the above  $r_2$ , the calculation must be repeated with

$$r_3 = 20 , \quad F_3 = 976.64 ,$$

and the definitive value  $F_0 = 977.04$  is obtained. This value then gives the smallest circle.

The diameter of this smallest circle, and thus the maximum value of  $d$ , might be considered a measure of the quality of the objective. However, it is more correct to use as this measure a mean value of the  $d$  values of all zones, because it is indeed possible that the above maximum value is based upon only a very narrow and weakly illuminated zone, which contains only a small fraction of the total light. The mean value mentioned is expressed, in terms of the light amount falling on the individual zones, in the form  $\Sigma r d / \Sigma r$ . The mean value thus found for the circle is further expressed in fractions of the focal length, to permit direct comparison of objectives of different dimensions with one another, and it is multiplied by 100,000 to obtain reasonable sizes of numbers. If this number thus calculated (and characteristic of any objective) is called  $T$ , there is finally obtained

$$T = \frac{100,000}{F_0} \frac{\Sigma r d}{\Sigma r} = \frac{200,000}{F_0^2} \frac{\Sigma r^2 (F - F_0)}{\Sigma r} , \tag{22}$$

in which only the absolute amounts, without regard to sign, are to be substituted for the quantity  $F - F_0$ . The quantity  $T$  is the mean diameter of the geometric diffusion circle expressed in parts of  $F_0/100,000$

and  $2.0626$  seconds  $\cdot T$  of the apparent diameter of this circle in arc seconds. The quantity  $T$  is identical with the "technical constant" of the objective first introduced by Lehmann<sup>17</sup>. Later<sup>18</sup> he multiplied this expression by the aperture ratio to permit comparison of objectives of different types. This is scarcely an improvement, however, because by this the above-mentioned simple significance of  $T$  is lost and the comparison of different types must, of course, be done in accordance with other viewpoints.

Calculation from Equation (22) gives for the objective studied

$$T = 1.023.$$

The mean diameter of the geometric diffusion circle is thus  $1.023 F_0 \cdot 10^{-5} = 0.010$  mm or 2.11 seconds.

According to my experience, objectives for which  $T$  exceeds the value 1.5 can be considered only "moderately good." For good objectives  $T$  is between 1.5 and 0.5, and for extremely good objectives  $T$  is less than 0.5. For the ideal objective, free of zonal aberration,  $T$  would be 0. It would be very desirable if general and precise objective studies, especially at the observatories, were to be conducted according to the methods given here and the aberration curves and values of  $T$  found were to be published, because it is only on the basis of extensive observation material that a completely adequate classification of objectives can be developed.

PRECEDING PAGE BLANK NOT FILMED.

LITERATURE CITED

1. Monatsber, d. Berl. Akad. (Monthly Report of the Berlin Academy), 1880, p. 433.
2. Bessel, Astronomische Untersuchungen (Astronomical Studies), Vol. 1, 1841, p. 103.
3. L. Foucault, CONSTRUCTION OF A SILVERED GLASS TELESCOPE, Ann. de l'Observatoire de Paris (Journal of the Paris Observatory), Vol. 5, 1859, p. 197.
4. H. Schroeder, Die Elemente der photographischen Optik (Fundamentals of Photographic Optics), Berlin, 1891, p. 171.
5. S. Czapski, ABBE'S METHODS AND APPARATUS FOR DETERMINATION OF FOCAL LENGTH, Zeitschrift für Instrumentenkunde, Vol. 12, 1892, p. 185.
6. J. Wilsing, THE EFFECT OF SPHERICAL DEVIATIONS OF THE WAVE FRONT ON THE LIGHT INTENSITY OF TELESCOPE OBJECTIVES, Publ. d. Astrophys. Observ. zu Potsdam (Publications of the Potsdam Astronomical Observatory), Vol. 15, No. 48, 1903.
7. G. Eberhard, DETERMINATION OF THE COLOR CURVE OF OBJECTIVES OF MEDIUM FOCAL LENGTH, Zeitschrift für Instrumentenkunde, Vol. 23, 1903, p. 82, THE HARMFUL EFFECT OF CEMENTING OBJECTIVES, p. 274.
8. H. Lehmann, THE APPLICATION OF THE HARTMANN METHOD TO ZONAL TESTING OF ASTRONOMIC OBJECTIVES, Zeitschrift für Instrumentenkunde, Vol. 22, 1902, pp. 103 and 325, Vol. 23, 1903, p. 289.
9. J. Hartmann, A SERIES OF FILTERS FOR PRODUCTION OF HOMOGENEOUS LIGHT, Zeitschr. f. wissensch. Photogr. (Magazine for Scientific Photography), Vol. 1, 1903, p. 259.
10. H. Lehmann, Zeitschr. f. Instrumentenkunde, Vol. 23, 1903, p. 290.
11. H. Lehmann, Zeitschr. f. Instrumentenkunde, Vol. 22, 1902, p. 325.

12. H. Lehmann, Zeitschr. f. Instrumentenkunde, Vol. 22, 1902, p. 326.
13. Ch. Féry, NEW METHOD FOR DETERMINING THE CONSTANTS OF LENSES, Journ. de phys. (Physics Journal), Vol. 2, 1903, p. 755.
14. Gauss, Dioptrische Untersuchungen (Dioptric Studies), p. 2.
15. Sitzungsber. d. Wiener Akad. (Meeting Reports of the Viennese Academy), Vol. 112, IIa, 1903, p. 1057.
16. K. Strehl, ZONAL ABERRATION AND WAVE SURFACES, Zeitschr. f. Instrumentenkunde, Vol. 20, 1900, p. 266.
17. Zeitsch. f. Instrumentenkunde, Vol. 22, 1902, p. 108.
18. Zeitsch. f. Instrumentenkunde, Vol. 22, 1902, p. 327.



## DISTRIBUTION

	No. of Copies
Defense Documentation Center Cameron Station Alexandria, Virginia 22314	20
Central Intelligence Agency ATTN: OCR/DD-Standard Distribution Washington, D. C. 20505	4
Foreign Science and Technology Center U. S. Army Missile Command ATTN: Mr. Shapiro Washington, D. C. 20315	3
NASA Scientific and Technical Information Facility ATTN: Acquisitions Branch (S-AK/DL) P. O. Box 33 College Park, Maryland 20740	5
Division of Technical Information Extension U. S. Atomic Energy Commission P. O. Box 62 Oak Ridge, Tennessee 37830	1
Foreign Technology Division ATTN: Library Wright-Patterson Air Force Base, Ohio 45400	1
USACDC-LnO	1
MS-T, Mr. Wiggins	5
AMSMI-D	1
-XE, Mr. Lowers	1
-XS, Dr. Carter	1
-Y	1
-R, Mr. McDaniel	1
-RB, Mr. Croxton	1
-RBLD	10
-RBT	8
-RAP	1

## DOCUMENT CONTROL DATA - R&amp;D

(Security classification of title, body of abstract and indexing annotation must be entered when the overall report is classified)

1. ORIGINATING ACTIVITY (Corporate author) Redstone Scientific Information Center Research and Development Directorate U. S. Army Missile Command Redstone Arsenal, Alabama 35809		2a. REPORT SECURITY CLASSIFICATION Unclassified	
		2b. GROUP N/A	
3. REPORT TITLE STUDY OF OBJECTIVES Zeitschrift für Instrumentenkunde, <u>24</u> , No. 1, 1-21 and <u>24</u> , No. 2, 33-47 (1904)			
4. DESCRIPTIVE NOTES (Type of report and inclusive dates) Translated from the German			
5. AUTHOR(S) (Last name, first name, initial)  Hartmann, J.			
6. REPORT DATE 24 January 1967		7a. TOTAL NO. OF PAGES 55	7b. NO. OF REFS 18
8a. CONTRACT OR GRANT NO. N/A		9a. ORIGINATOR'S REPORT NUMBER(S)  RSIC-639	
b. PROJECT NO. N/A		9b. OTHER REPORT NO(S) (Any other numbers that may be assigned this report) AD _____	
c.			
d.			
10. AVAILABILITY/LIMITATION NOTICES Each transmittal of this document outside the agencies of the U. S. Government must have prior approval of this Command, ATTN: AMSMI-RBT.			
11. SUPPLEMENTARY NOTES  None		12. SPONSORING MILITARY ACTIVITY  Same as No. 1	
13. ABSTRACT The author understands the test of a telescope objective to be the determination of its focal length, chromatic and spherical aberration, or zonal aberration and astigmatism on the axis. To this might be added testing for extra-axial images, transmittance of the glass, and measurement of the free aperture, as well as possible notes on the position of reflex images, on centering and purity of the lenses, and similar matters. The test of a small objective of 80-mm aperture and 1-m focal length with the aid of terrestrial light sources is described first; small modifications of the method which are necessary in the testing of astronomical objectives with the aid of stars are also given. The test is performed in the actual mounting of the objective, which in the case at hand is a brass tube. To the eyepiece of this tube one can connect, by means of a bayonet joint, a filar micrometer, a photographic camera, or a small slit spectrograph. The setting can be read to 0.1 mm with a vernier. The study of the objective can be broken down as follows: determination of the position of the focal points of all rays in terms of the graduation of the adjustment (this is called focusing), and measurement of the distance of this graduation, either from a fixed point of the objective mount—which gives the combining distances—or from the second principal point of the objective, in which case the focal lengths are obtained.			

14. KEY WORDS	LINK A		LINK B		LINK C	
	ROLE	WT	ROLE	WT	ROLE	WT
Extrafocal measurements Astigmatism Filar micrometer Chromatic aberration White light Extrafocal image Color zone Gaussian theory						

INSTRUCTIONS

1. **ORIGINATING ACTIVITY:** Enter the name and address of the contractor, subcontractor, grantee, Department of Defense activity or other organization (*corporate author*) issuing the report.

2a. **REPORT SECURITY CLASSIFICATION:** Enter the overall security classification of the report. Indicate whether "Restricted Data" is included. Marking is to be in accordance with appropriate security regulations.

2b. **GROUP:** Automatic downgrading is specified in DoD Directive 5200.10 and Armed Forces Industrial Manual. Enter the group number. Also, when applicable, show that optional markings have been used for Group 3 and Group 4 as authorized.

3. **REPORT TITLE:** Enter the complete report title in all capital letters. Titles in all cases should be unclassified. If a meaningful title cannot be selected without classification, show title classification in all capitals in parenthesis immediately following the title.

4. **DESCRIPTIVE NOTES:** If appropriate, enter the type of report, e.g., interim, progress, summary, annual, or final. Give the inclusive dates when a specific reporting period is covered.

5. **AUTHOR(S):** Enter the name(s) of author(s) as shown on or in the report. Enter last name, first name, middle initial. If military, show rank and branch of service. The name of the principal author is an absolute minimum requirement.

6. **REPORT DATE:** Enter the date of the report as day, month, year; or month, year. If more than one date appears on the report, use date of publication.

7a. **TOTAL NUMBER OF PAGES:** The total page count should follow normal pagination procedures, i.e., enter the number of pages containing information.

7b. **NUMBER OF REFERENCES:** Enter the total number of references cited in the report.

8a. **CONTRACT OR GRANT NUMBER:** If appropriate, enter the applicable number of the contract or grant under which the report was written.

8b, 8c, & 8d. **PROJECT NUMBER:** Enter the appropriate military department identification, such as project number, subproject number, system numbers, task number, etc.

9a. **ORIGINATOR'S REPORT NUMBER(S):** Enter the official report number by which the document will be identified and controlled by the originating activity. This number must be unique to this report.

9b. **OTHER REPORT NUMBER(S):** If the report has been assigned any other report numbers (*either by the originator or by the sponsor*), also enter this number(s).

10. **AVAILABILITY/LIMITATION NOTICES:** Enter any limitations on further dissemination of the report, other than those imposed by security classification, using standard statements such as:

- (1) "Qualified requesters may obtain copies of this report from DDC."
- (2) "Foreign announcement and dissemination of this report by DDC is not authorized."
- (3) "U. S. Government agencies may obtain copies of this report directly from DDC. Other qualified DDC users shall request through \_\_\_\_\_."
- (4) "U. S. military agencies may obtain copies of this report directly from DDC. Other qualified users shall request through \_\_\_\_\_."
- (5) "All distribution of this report is controlled. Qualified DDC users shall request through \_\_\_\_\_."

If the report has been furnished to the Office of Technical Services, Department of Commerce, for sale to the public, indicate this fact and enter the price, if known.

11. **SUPPLEMENTARY NOTES:** Use for additional explanatory notes.

12. **SPONSORING MILITARY ACTIVITY:** Enter the name of the departmental project office or laboratory sponsoring (*paying for*) the research and development. Include address.

13. **ABSTRACT:** Enter an abstract giving a brief and factual summary of the document indicative of the report, even though it may also appear elsewhere in the body of the technical report. If additional space is required, a continuation sheet shall be attached.

It is highly desirable that the abstract of classified reports be unclassified. Each paragraph of the abstract shall end with an indication of the military security classification of the information in the paragraph, represented as (TS), (S), (C), or (U).

There is no limitation on the length of the abstract. However, the suggested length is from 150 to 225 words.

14. **KEY WORDS:** Key words are technically meaningful terms or short phrases that characterize a report and may be used as index entries for cataloging the report. Key words must be selected so that no security classification is required. Identifiers, such as equipment model designation, trade name, military project code name, geographic location, may be used as key words but will be followed by an indication of technical context. The assignment of links, rules, and weights is optional.